



**Untangling a Gordian knot: the role of a GluCl3 I321T mutation in abamectin resistance in *Tetranychus urticae***

Journal:	<i>Pest Management Science</i>
Manuscript ID	PM-20-0994.R1
Wiley - Manuscript type:	Research Article
Date Submitted by the Author:	03-Nov-2020
Complete List of Authors:	Xue, Wenxin; Ghent University, Department of Plants and Crops Mermans, Catherine; Ghent University, Department of Plants and Crops Papapostolou, Kyriaki-Maria; Foundation of Research and Technology Hellas, Institute of Molecular Biology & Biotechnology; University of Crete Voutes Campus, Department of Biology Lamprousi, Mantha ; Foundation of Research and Technology Hellas, Institute of Molecular Biology & Biotechnology; University of Crete Voutes Campus, Department of Biology Christou, Iason-Konstantinos ; Foundation of Research and Technology Hellas, Institute of Molecular Biology & Biotechnology; University of Crete Voutes Campus, Department of Biology Inak, Emre; Ankara University, Department of Plant Protection Douris, Vassilis; Foundation of Research and Technology Hellas, Institute of Molecular Biology & Biotechnology; University of Ioannina, Department of Biological Applications and Technology Vontas, John; Foundation of Research and Technology Hellas, Institute of Molecular Biology & Biotechnology; Agricultural University of Athens, Department of Crop Science Dermauw, Wannes; Ghent University, Department of Plants and Crops Van Leeuwen, Thomas; Ghent University, Department of Plants and Crops
Key Words:	avermectin, ivermectin, arthropoda, GluCl, Rdl, two-electrode voltage-clamp electrophysiology

SCHOLARONE™  
Manuscripts

1  
2  
3 **1 Untangling a Gordian knot: the role of a GluCl3 I321T mutation in**  
4 **2 abamectin resistance in *Tetranychus urticae***  
5  
6  
7  
8

9 4 Wenxin Xue<sup>1</sup>, Catherine Mermans<sup>1</sup>, Kyriaki-Maria Papapostolou<sup>2,3</sup>, Mantha  
10 5 Lamprousi<sup>2,3</sup>, Iason-Konstantinos Christou<sup>2,3</sup>, Emre Inak<sup>4</sup>, Vassilis Douris<sup>2,5</sup>, John  
11 6 Vontas<sup>2,6</sup>, Wannes Dermauw<sup>1,\*</sup>, Thomas Van Leeuwen<sup>1,\*</sup>  
12  
13  
14

15  
16 8 <sup>1</sup> Department of Plants and Crops, Faculty of Bioscience Engineering, Ghent  
17 9 University, Coupure links 653, 9000, Ghent, Belgium

18  
19 10 <sup>2</sup> Institute of Molecular Biology & Biotechnology, Foundation for Research &  
20 11 Technology Hellas, 100 N. Plastira Street, GR-700 13, Heraklion Crete, Greece

21  
22 12 <sup>3</sup> Department of Biology, University of Crete, 70013, Heraklion, Crete, Greece

23  
24 13 <sup>4</sup> Department of Plant Protection, Faculty of Agriculture, Ankara University, Diskapi,  
25 14 06110 Ankara, Turkey.

26  
27 15 <sup>5</sup> Department of Biological Applications and Technology, University of Ioannina, 451  
28 16 10 Ioannina, Greece

29  
30 17 <sup>6</sup> Laboratory of Pesticide Science, Department of Crop Science, Agricultural  
31 18 University of Athens, 75 Iera Odos Street, 11855, Athens, Greece  
32  
33  
34  
35

36  
37 20 \*corresponding author:

38 21 Thomas Van Leeuwen, e-mail: [thomas.vanleeuwen@ugent.be](mailto:thomas.vanleeuwen@ugent.be)  
39 22 postal address: Coupure links 653, 9000 Ghent  
40 23 telephone number: +32(0)9 264 61 43

41  
42 24 Wannes Dermauw, e-mail: [wannes.dermauw@ugent.be](mailto:wannes.dermauw@ugent.be)  
43 25 postal address: Coupure links 653, 9000 Ghent  
44 26 telephone number: +32(0)9 264 61 92  
45

46 27  
47  
48 28 e-mail address of each author:  
49 29  
50 30  
51 31  
52 32  
53 33  
54 34  
55 35  
56 36  
57 37  
58 38  
59  
60

## 39 **Abstract**

### 40 **BACKGROUND**

41 The cys-loop ligand-gated ion channels, including the glutamate-gated chloride  
42 channel (GluCl) and GABA-gated chloride channel (Rdl) are important targets for drugs  
43 and pesticides. The macrocyclic lactone abamectin primarily targets GluCl and is  
44 commonly used to control the spider mite *Tetranychus urticae*, an economically  
45 important crop pest. However, abamectin resistance has been reported for multiple *T.*  
46 *urticae* populations worldwide, and in several cases was associated with the mutations  
47 G314D in *GluCl1* and G326E in *GluCl3*. Recently, an additional I321T mutation in  
48 *GluCl3* was identified in several abamectin resistant *T. urticae* field populations. Here,  
49 we aim to functionally validate this mutation and determine its phenotypic strength.

### 51 **RESULTS**

52 The *GluCl3* I321T mutation was introgressed into a *T. urticae* susceptible background  
53 by marker-assisted backcrossing, revealing contrasting results in phenotypic strength,  
54 ranging from almost none to 50-fold. Next, we used CRISPR-Cas9 to introduce I321T,  
55 G314D and G326E in the orthologous *Drosophila GluCl*. Genome modified flies  
56 expressing GluCl I321T were threefold less susceptible to abamectin, while CRISPRed  
57 G314D and G326E flies were lethal. Last, functional analysis in *Xenopus* oocytes  
58 revealed that the I321T mutation might reduce GluCl3 sensitivity to abamectin, but also  
59 that all three *T. urticae* Rdl are affected by abamectin [at high concentrations](#).

### 61 **CONCLUSION**

62 Three different techniques were used to characterize the role of I321T in GluCl3 in  
63 abamectin resistance and, combining all results, our analysis suggests that the I321T  
64 mutation has a complex role in abamectin resistance. [Given the reported subtle effect,](#)  
65 [additional synergistic factors in resistance warrant more investigation.](#)

67 **Keywords:** avermectin, ivermectin, arthropoda, GluCl, Rdl, two-electrode voltage-  
68 clamp electrophysiology

## 69 1 INTRODUCTION

70 Macrocytic lactones such as avermectins and milbemycins are natural fermentation  
71 products of *Streptomyces* bacteria. They exhibit strong insecticidal, nematicidal, and  
72 acaricidal activity with low toxicity in mammals and have been widely used in pest  
73 control and as anthelmintics in animal and human health for several decades.<sup>1–5</sup>  
74 Macrocytic lactones are neurotoxins known to act on cys-loop ligand-gated ion  
75 channels (LGICs). These channels contain five homologous subunits, where each  
76 subunit consists of a large N-terminal extracellular domain, four hydrophobic alpha-  
77 helical transmembrane segments (TMs), an intracellular loop between TM3 and TM4  
78 and a short extracellular C terminus to form a central ion channel lining (Fig. 1a).<sup>6–9</sup> In  
79 invertebrates, the glutamate-gated chloride channel (GluCl), GABA-gated chloride  
80 channel (GABACl, also known as Resistance to dieldrin (Rdl)), the histamine-gated  
81 chloride channel (HisCl) and the pH-sensitive chloride channel (pHCl) belong, amongst  
82 others, to the cys-loop LGIC family.<sup>2,10–14</sup> In *Caenorhabditis elegans* six GluCl and one  
83 Rdl gene have been identified,<sup>7,8,15,16</sup> while most insects, except Lepidoptera and  
84 aphids, only have a single GluCl and Rdl gene. Genome sequencing of the spider mite  
85 *Tetranychus urticae* and the honeybee mite *Varroa destructor*, revealed the presence  
86 of five GluCl and three Rdl genes in *T. urticae*, while three Rdl genes have been found  
87 in *V. destructor*.<sup>14,17–21</sup> The GluCl has an important role in the nervous system,  
88 including modulation of locomotion, regulation of feeding and mediation of sensory  
89 inputs and is the primary target of macrocytic lactones, while Rdl is considered as a  
90 secondary target of these compounds.<sup>15,22–26</sup> Fuse et al., for example, showed that the  
91 EC<sub>50</sub> of ivermectin, an avermectin, was more than 150-fold larger for *Musca domestica*  
92 Rdl than for GluCl.<sup>26</sup> Of peculiar note, cys-loop channels, sensitive to ivermectin,  
93 consisting of both GluCl and Rdl subunits have previously been reported.<sup>12,27,28</sup>

94 The spider mite *T. urticae* is a highly polyphagous pest and develops resistance  
95 very rapidly.<sup>29,30</sup> A frequently used compound to control *T. urticae* is abamectin, a  
96 mixture of avermectins containing a minimum of 80% avermectin B<sub>1a</sub> and maximum 20%  
97 avermectin B<sub>1b</sub>. Due to its extensive application for decades, increasing field abamectin  
98 resistance in *T. urticae* has been reported.<sup>31–36</sup> Backcrossing experiments and F<sub>2</sub>  
99 screen showed that two mutations, G314D in *GluCl1* and G326E in *GluCl3*, were  
100 associated with abamectin resistance in *T. urticae*.<sup>14,37</sup> Based on the crystal structure  
101 of the *C. elegans* GluCl $\alpha$ -subunit and its binding-mode to ivermectin, a residue in the

1  
2  
3 102 third transmembrane region (TM3), equivalent to the position of the above two  
4  
5 103 mutations, was likely involved in the formation of the allosteric site and located closest  
6  
7 104 to ivermectin.<sup>7</sup> In addition, functional validation using two electrode voltage-clamp  
8  
9 105 electrophysiology and *Xenopus* oocytes also revealed that a G326E substitution in *T.*  
10  
11 106 *urticae* GluCl3 completely abolished the agonistic activity of abamectin.<sup>38</sup> Further, an  
12  
13 107 identical substitution at an equivalent position in *Plutella xylostella* GluCl reduced the  
14  
15 108 sensitivity to abamectin by about 500-fold,<sup>39</sup> while a G329D substitution (corresponding  
16  
17 109 to G314D in *T. urticae* GluCl1) in *Haemonchus contortus* GluCl, abolished binding with  
18  
19 110 the macrocyclic lactone milbemycin A<sub>4</sub>.<sup>40</sup>

20  
21 111 Recently, a target-site (GluCl) screening of 32 European field *T. urticae* strains,  
22  
23 112 revealed the presence of a potential new target-site mutation, I321T in *GluCl3*, in four  
24  
25 113 abamectin resistant strains.<sup>36</sup> This mutation was also found in another abamectin  
26  
27 114 resistant strain from Peloponnese, Greece in a recently published paper of  
28  
29 115 Papapostolou et al. 2020.<sup>41</sup> This mutation is adjacent to A309V, a previously reported  
30  
31 116 abamectin resistance associated mutation in *P. xylostella*.<sup>39</sup> In addition, two other  
32  
33 117 mutations V327G (adjacent to the important G326 residue) and L329F were also found  
34  
35 118 in *GluCl3* of a strain exhibiting an around 500-fold resistance ratio (RR). L329  
36  
37 119 corresponds to M345 of *C. elegans* GluCl $\alpha$ , a residue predicted to be involved in  
38  
39 120 ivermectin binding;<sup>7</sup> while two substitutions at a position equivalent to L329F (L315F  
40  
41 121 and L319F in GluCl of *M. domestica* and *Bombyx mori*, respectively) also showed  
42  
43 122 reduced sensitivity to ivermectin.<sup>42,43</sup> However, none of these recently identified  
44  
45 123 mutations (I321T, V327G and L329F) have been functionally validated in *T. urticae*.  
46  
47 124 Characterizing the properties of these mutations could help in understanding the  
48  
49 125 macrocyclic lactone resistance mechanisms in *T. urticae* and, in the long term, might  
50  
51 126 aid in designing effective pest management strategies. In this study, the main aim is to  
52  
53 127 characterize the I321T mutation in *GluCl3*. First, we performed electrophysiological  
54  
55 128 analyses to clarify the effect of abamectin on GluCl3 wild-type, I321T GluCl3 and Rdl  
56  
57 129 in *T. urticae*. Next, marker-assisted back-crossing was used to introduce the mutation  
58  
59 130 into a *T. urticae* line with a susceptible genetic background, and the relative  
60  
131 contribution of the mutation to abamectin resistance was assessed. Finally, CRISPR-  
132 Cas9 technology was used to introduce the I321T mutation in the *Drosophila* GluCl  
133 homologue, and the effect of I321T on abamectin resistance was compared against  
134 the nos.Cas9 stock and G314D and G326E flies.

## 135 2 MATERIALS AND METHODS

### 136 2.1 Mite strains

137 The abamectin susceptible strain SR6 was collected from tomato plants in Italy in 2017.  
138 This strain was inbred by six rounds of mother-son mating as previously described in  
139 Bryon et al. 2017 and screened for the presence of mutations in *GluCl1/2/3/4/5* TM3  
140 and *Rdl1/2/3* TM2/TM3 regions (see 2.2).<sup>44</sup> The abamectin resistant strain IT6 has  
141 been previously described and of all five *GluCl* genes only *GluCl3* carried an I321T  
142 mutation,<sup>36</sup> while the TM2/TM3 region of *Rdl1/2/3* was screened in this study (see 2.2.)  
143 The abamectin resistant strain TR2 (corresponding to sample number 2 in Inak et al.  
144 2019) has been previously described and lacks the previously documented abamectin  
145 resistance mutations, G314D in *GluCl1* and G326E in *GluCl3*.<sup>45</sup> The TM3 region of  
146 *GluCl2/4/5*, I321T mutation in *GluCl3* and TM2/TM3 region *Rdl1/2/3* of TR2 were  
147 screened in this study (see 2.2). In our previous study, the strains IT1, IT5 and ES1  
148 were screened for the presence of mutations in TM3 of *GluCl1/2/3/4/5* <sup>36</sup> while the  
149 TM2/TM3 regions of *Rdl1/2/3* of these strains were screened in this study. Furthermore,  
150 all *GluCl* and *Rdl* genes from MR-VL from Belgium<sup>46</sup>, were also screened in this study.  
151 Detailed information of all strains can be found in Table S1. All *T. urticae* strains were  
152 maintained on non-sprayed kidney bean leaves (*Phaseolus vulgaris* L. cv. "Prelude")  
153 under laboratory conditions (25±1°C, 60% relative humidity, and 16:8 hr light: dark  
154 photoperiod).

### 155 2.2 Survey of genotypes in *GluCl* TM3 and *Rdl* TM2/TM3 regions

156 Genomic DNA (gDNA) of strains IT1, IT5, IT6, ES1, MR-VL and SR6 was extracted  
157 from approximately 200 *T. urticae* female adults as described earlier by Van Leeuwen  
158 et al. (2008). gDNA of the TR2 strain was extracted from approximately 100 adult  
159 female mites with the Qiagen DNeasy Blood & Tissue Kit following the manufacturer's  
160 instructions. Quality and quantity of DNA were checked via a spectrophotometer  
161 (Thermo Scientific NanoDrop 2000 or a DeNovix DS-11 (DeNovix, Willmington, DE,  
162 USA)). PCR amplification of the TM3 regions from five *GluCl* genes and TM2/TM3  
163 fragments from three *Rdl* genes was performed as described by Dermauw et al..<sup>14</sup>  
164 Primers used for PCR are listed in Table S3. PCR-products were purified using E.Z.N.A.  
165 Cycle Pure Kit (Omega Bio-Tek) and were sequenced (LGC genomics, Germany). All  
166 sequenced data was analysed using BioEdit version 7.0.5.2..<sup>47</sup>

## 167 **2.3 Toxicity bioassays**

168 Toxicity bioassays were carried out with commercially formulated abamectin (Vertimec  
169 18 g a.i./L EC or Agrimec 18 g a.i./L EC). At least five concentrations (causing between  
170 20 and 80% mortality) were tested in four replicates and blank controls were sprayed  
171 with deionised water only. For each replicate, about 20-30 young adult female mites  
172 were transferred to 9-cm<sup>2</sup> bean leaf disks and sprayed with serial pesticide dilutions at  
173 1 bar pressure. For IT6 and congenic lines (2.4), a Cornelis spray tower was used for  
174 spraying leaf disks and 0.8 mL of pesticide dilution was applied to obtain a  $1.5 \pm 0.05$   
175 mg aqueous acaricide deposit cm<sup>-2</sup>.<sup>45,46,48</sup> For TR2 and congenic lines (2.4), a Potter  
176 spray tower (Burkard Scientific Ltd, Uxbridge, UK) was used for spraying and 2 mL of  
177 acaricide dilution was applied to obtain a  $1.95 \pm 0.05$  mg aqueous acaricide deposit  
178 cm<sup>-2</sup>. LC<sub>50</sub> and LC<sub>90</sub> values and their 95% **confidence intervals (CIs)** were determined  
179 with PoloPlus (LeOra Software, Berkeley, CA, USA, 2006).<sup>49</sup> **Resistance ratios (RRs)**  
180 **were considered significantly different when their 95% CI did not include the value 1.**<sup>50</sup>

## 181 **2.4 Backcrossing experiments**

### 182 **2.4.1 Establishment of congenic lines**

183 To assess the resistance levels associated with the I321T mutation, we used a marker  
184 assisted backcrossing approach to produce near-isogenic sister lines as previously  
185 outlined in Riga *et al.* 2017.<sup>51</sup> Briefly, a haploid male of a resistant strain (IT6= BC1 or  
186 TR2= BC2) was crossed with a virgin female of the susceptible strain SR6, in three  
187 and four replicates respectively. The resulting heterozygous virgin females of each  
188 replicate cross were backcrossed to susceptible males of SR6 and heterozygote  
189 genotypes (I321/T321) were identified by PCR and sequencing as described in section  
190 2.4.2. This process was repeated for seven generations. In the last generation,  
191 backcrossed heterozygous virgin females were crossed with their first-born sons,  
192 representing either the I321 or T321 genotype respectively, and resulting in congenic  
193 homozygous lines (with either the I321/I321 or T321/T321 genotype).

### 194 **2.4.2 Single mite DNA extraction and genotyping**

195 DNA from individual adult females was extracted using the Qiagen DNeasy Blood &  
196 Tissue Kit following the manufacturer instructions, or by homogenization in 20  $\mu$ L STE  
197 buffer (100 mM NaCl, 10 mM Tris- HCl and 1 mM EDTA) with 1 mg ml<sup>-1</sup> proteinase K  
198 (Sigma-Aldrich, Overijse, Belgium) and incubated for 30 min at 37 °C and 5 min at  
199 95 °C.<sup>51</sup> The primers used to amplify the TM3 of GluCl3 were as follows: 5'-3'

1  
2  
3 200 CCGGGTCAGTCTTGGTGTTA and 3'- 5' CACCACCAAGAACCTGTTGA.<sup>14</sup> Then  
4 201 standard PCR was conducted with single mite DNA. PCR products were purified and  
5 202 sequenced (LGC genomics, Germany and Macrogen Inc., Seoul, Korea). All  
6 203 sequenced data was analysed using BioEdit version 7.0.5.2.<sup>47</sup>

### 10 204 **2.4.3 Toxicity bioassays of congenic lines**

11 205 Toxicity bioassays with abamectin were carried out as described in 2.3.

## 15 206 **2.5 CRISPR-Cas9 genome editing in *Drosophila***

### 17 207 **2.5.1 *Drosophila* stocks**

18 208 Genome modification of *Drosophila* was performed in the strain y1 M{nos-Cas9.P} ZH-  
19 209 2A w\*,<sup>52</sup> in which Cas9 is expressed under the control of the *nos* promoting element  
20 210 (strain #54591 at the Bloomington *Drosophila* stock center, hereafter referred to as  
21 211 nos.Cas9). We also used a balancer stock for the third chromosome (*yw*; TM3 Sb e /  
22 212 TM6B Tb Hu e), hereafter referred to as TM3/TM6B. Flies were cultured under  
23 213 laboratory conditions (25 °C, 60-70% relative humidity, and 12:12 hr light: dark  
24 214 photoperiod) and fed on a standard fly diet.

### 31 215 **2.5.2 *Drosophila* DNA purification and amplification**

32 216 DNA was purified from *Drosophila* by DNAzol® (MRC) according to manufacturer  
33 217 instructions. PCR amplification with relevant primer pairs (Table S3) was performed  
34 218 with Taq DNA Polymerase (MINOtech BIOTECHNOLOGY) and the conditions used  
35 219 were 94 °C for 2 min, followed by 35 cycles of denaturation at 94°C for 45 sec,  
36 220 annealing at 57 °C (generic primers) or 51 °C (specific primers) for 30 sec, and  
37 221 extension at 72 °C for 30 sec followed by a final extension step at 72 °C for 5 min.

### 44 222 **2.5.3 Genomic engineering strategy**

45 223 An *ad hoc* CRISPR-Cas9 genomic engineering strategy was designed in order to  
46 224 generate the mutations of interest (GluCl1 G314D, GluCl3 G326E and GluCl3 I321T,  
47 225 *T. urticae* numbering) at the *GluCl* gene (CG7535) of *D. melanogaster* (Fig. S1).

48 226 In order to identify possible variations from the published genome sequence,  
49 227 two sets of primers pairs were used (GluExFw/GluExRv and GluInFw/GluInRv, Table  
50 228 S3) and a nos.Cas9 DNA template to amplify and sequence a 1771 bp DNA fragment  
51 229 corresponding to the genomic region 3R: 19,763,419-19,765,189 (BDGP6.28 genome  
52 230 assembly) encompassing exons 8 and 9 of GluCl (Fig. S1). Potential CRISPR targets  
53 231 in the region of interest were identified using the online tool Optimal Target Finder<sup>53</sup>



232 (<http://tools.flycrispr.molbio.wisc.edu/targetFinder/>) and a target with no predicted off-  
233 target hits was selected.

234 A relevant sgRNA expressing plasmid was generated using vector pU6-BbsI  
235 chiRNA<sup>54</sup> by sub cloning a double stranded DNA oligo (generated by annealing sense  
236 and antisense sgRNA oligos (Table S3). To facilitate Homologous Directed Repair  
237 (HDR), three donor plasmids were synthesized *de novo* (donorI321T, donorG314D  
238 and donor G326E (Genscript, NJ, USA)) containing two ~800 bp homology arms  
239 flanking the CRISPR target. The donor sequences correspond to the genomic region  
240 3R: 19,763,457-19,765,164 and contain the non-synonymous substitution that  
241 generates the relevant mutations as well as certain synonymous mutations  
242 incorporated for diagnostic purposes or to avoid cleavage of the donor plasmid by the  
243 CRISPR/Cas9 machinery. Plasmid donorG314D contained the non-synonymous  
244 GGC→GAC substitution (leading to the G314D mutation), as well as synonymous  
245 mutations to abolish an existing ClaI restriction site and introduce a new MluI restriction  
246 site (Fig. S2a). Similarly, plasmid donorG326E contained at the same site the non-  
247 synonymous GGC→GAG substitutions (leading to the G326E mutation), as well as  
248 synonymous mutations to abolish an existing XhoI restriction site and introduce a new  
249 Accl restriction site (Fig. S2b), while plasmid donorI321T contained the non-  
250 synonymous ATC→ACC substitution (leading to the I321T mutation and abolishment  
251 of ClaI) as well as certain synonymous mutations to introduce MluI and inhibit  
252 recognition and cleavage of the plasmid by CRISPR/Cas9 (Fig. S2c). Note that the  
253 G→D or G→E mutations occur at the same position (G312 in *Drosophila* GluCI) for  
254 donorG314D and donorG326E, respectively.

#### 255 **2.5.4 Generation and screening of genome modified flies**

256 Preblastoderm nos.Cas9 embryos were injected with a plasmid mixture containing 75  
257 ng/  $\mu$ L of sgRNA plasmid and 100 ng/  $\mu$ L of donor plasmid in injection buffer (2 mM  
258 Sodium phosphate pH 6.8-7.8, 100 mM KCl). Injected G<sub>0</sub> adults were back-crossed to  
259 nos. Cas9 and G<sub>1</sub> progeny was initially screened *en masse* to identify crosses that had  
260 produced G<sub>1</sub> flies that underwent HDR events (Fig. S3a). Screening was performed by  
261 DNA extraction from batches of ~30 individuals per vial, digesting ~2  $\mu$ g of total DNA  
262 with ClaI (for G314D and I321T) or XhoI (for G326E) in order to preferentially digest  
263 wild-type alleles but not the genome modified alleles that contain the donor sequence  
264 where the corresponding site is absent, and using ~30 ng of the digested DNA as

1  
2  
3 265 template for amplification. Screening was performed either with a “generic” primer pair  
4  
5 266 yielding a 489 bp product that was further digested with *MluI* (for G314D and I321T) or  
6  
7 267 *AccI* (for G326E) that were introduced into the genome modified allele, or in the case  
8  
9 268 of I321T with a “specific” primer combination (*Dmel\_GluCl\_generic\_F* /  
10 269 *Dmel\_GluCl\_specific\_R*, Table S3) that generates a diagnostic fragment (429 bp) in  
11  
12 270 the presence of the modified allele.

13  
14 271 In case the presence of genome modified alleles was indicated in the pool,  
15 272 individual  $G_1$  flies from the same original cross were outcrossed with nos.Cas9 flies  
16  
17 273 and after generating progeny ( $G_2$ ), they were screened individually to identify crosses  
18  
19 274 bearing genome modified alleles. Several lines originating from positive  $G_1$  flies were  
20  
21 275 established, and individual  $G_2$  flies (expected to be heterozygous for the mutant allele  
22  
23 276 at a 50% ratio) were balanced against a TM3 / TM6B balancer strain and then  
24  
25 277 individually screened (Fig. S3b) to select crosses generating  $G_3$  progeny containing  
26  
27 278 the genome modified allele against the balancer chromosome. Then, single balanced  
28  
29 279  $G_3$  flies were back-crossed with the same balancer fly stock and following a final  
30  
31 280 molecular screening, adults with *Stubble* phenotype from two positive lines  
32  
33 281 (heterozygous for the mutation) were collected and crossed among themselves to  
34  
35 282 generate two homozygous strains bearing the I321T mutation. The established lines  
36  
37 283 were sequence verified (Fig. S3c). Sequencing reactions were performed at CeMIA  
38  
39 284 sequencing facility (CEMIA, S.A., Greece).

### 38 285 **2.5.5 Bioassays**

40 286 Abamectin was used for toxicity bioassays as a commercial insecticide formulation  
41  
42 287 (Vertimec 18 g a.i./L EC). Bioassays were performed as previously described.<sup>55</sup> Briefly,  
43  
44 288 2nd instar larvae were collected and transferred in batches of 20 into new vials  
45  
46 289 containing fly food supplemented with different insecticide concentrations. Total  
47  
48 290 development time was monitored for a period of 10-15 days for each applied insecticide  
49  
50 291 concentration, and pupation efficiency was used as a proxy for survival. Five to six  
51  
52 292 insecticide concentrations that cause 5-95% mortality (when applicable) were tested  
53  
54 293 in triplicates, together with relevant negative (no insecticide) controls for I321T and the  
55  
56 294 wild-type (nos.Cas9) strains.

### 56 295 **2.5.6 Statistical analyses**

57  
58 296 Observed mortality for each insecticide concentration was corrected for control (no  
59  
60 297 insecticide) mortality using Abbott’s formula.<sup>56</sup> The  $LC_{50}$  values and 95% confidence

1  
2  
3 298 intervals (CIs) were calculated via probit analysis using PoloPlus (LeOra Software,  
4 299 Berkeley, California), resistance ratios (RRs) were considered significantly different  
5 300 when the 95% CI of the RRs did not include the value 1.<sup>50</sup>  
6  
7  
8

## 9 301 **2.6 Two-electrode voltage-clamp electrophysiology**

### 11 302 **2.6.1 Vector construction and cRNA synthesis**

13 303 The TuGluCl3 I321T plasmid was generated by GenScript (Piscataway, New Jersey,  
14 304 USA) using site-directed mutagenesis and the TuGluCl3 WT plasmid, previously  
15 305 described in Mermans et al 2017, as template. The TuRdl# constructs were *in silico*  
16 306 generated in an identical way as TuGluCl3 WT constructs<sup>38</sup> except that the *T. urticae*  
17 307 GluCl3 coding sequence was replaced by either *T. urticae* Rdl1 (GenBank acc.  
18 308 AB567686.1, TuRdl1), Rdl2 (*tetur36g00580*, accessible at ORCAE<sup>57</sup>  
19 309 (<https://bioinformatics.psb.ugent.be/orcae/overview/Tetur>)), TuRdl2) and Rdl3  
20 310 (*tetur36g00590* accessible at ORCAE, TuRdl3) (also see File S1). All *T. urticae* Rdl  
21 311 coding sequences were codon optimized for *Xenopus* expression using the  
22 312 OptimumGene™-Codon Optimization software of GenScript. Next, TuRdl# constructs  
23 313 were synthesized *de novo* and ligated into a pUC57 plasmid by Genscript. After  
24 314 transformation into DH5α competent *Escherichia coli* (Invitrogen, Carlsbad, CA, USA)  
25 315 GluCl and Rdl plasmids were purified using the E.Z.N.A.® Plasmid DNA Mini Kit I  
26 316 (Qiagen, Germantown, MD, USA). The plasmids were linearized with NotI-HF  
27 317 restriction endonuclease (New England BioLabs Inc., Ipswich, MA, USA) followed by  
28 318 extraction using the phenol and chloroform method with ethanol precipitation<sup>58</sup>.  
29 319 Capped mRNAs were generated using the mMESSAGEMACHINE T7 transcription  
30 320 kit (Thermo Fischer Scientific, Waltham, MA, USA) according to manufacturer  
31 321 instructions. Synthesized cRNAs were purified with a RNeasy MinElute Cleanup Kit  
32 322 (Qiagen, Germantown, MD, USA), dissolved in nuclease-free water and stored at -  
33 323 80 °C until use.

### 50 324 **2.6.2 Oocyte injection and two-electrode voltage clamp electrophysiology**

51 325 Defolliculated, stage V–VI *X. laevis* oocytes were acquired from Ecocyte Bioscience  
52 326 (Castrop-Rauxel, Germany) in Tris-buffered Barth's solution (Ecocyte Bioscience).  
53 327 Oocytes were microinjected using a Nanoject III Programmable Nanoliter Injector  
54 328 (Drummond Scientific Co., Broomali, PA, USA) with 75 nL of cRNA solution (25–50 ng/  
55 329 μL) and incubated at 18 °C in sterile Barth's solution. Recordings were made 1–4 days  
56 330 post-cRNA injection. Two-electrode voltage-clamp (TEVC) measurements were  
57  
58  
59  
60

1  
2  
3 331 conducted with the fully automated Roboocyte2 (Multi Channel Systems MCS GmbH,  
4 332 Reutlingen, Germany); oocytes were held in a standard 96-well microtitre plate and  
5 333 impaled with two glass microelectrodes filled with 0.1 M KCl 1.5 M potassium acetate  
6 334 solution. Oocyte membrane potentials were fixed at -60mV throughout the experiment.

### 10 335 **2.6.3 Actions of L-glutamic acid and abamectin on wild type and I321T GluCl3**

11 336 Test solutions of L-glutamic acid monosodium salt monohydrate (CAS number 6106-  
12 337 04-3; Sigma–Aldrich) and abamectin (CAS number 71751-41-2, more than 80%  
13 338 avermectin B1a and less than 20% avermectin B1b; Sigma–Aldrich) were freshly  
14 339 prepared from stock solutions made with dimethyl sulfoxide (DMSO) and diluted with  
15 340 Normal Frog Ringer (NFR) solution (Ecocyte Bioscience). DMSO concentrations for  
16 341 test solutions did not exceed 1%. Dose-response curves to the natural agonist and  
17 342 compounds were obtained by sequential applications for 30 s of increasing  
18 343 concentrations with a 90s recorded wash-out (NFR) between applications for the  
19 344 channel to recover from desensitization. Abamectin application was preceded by L-  
20 345 glutamic acid (at EC<sub>50</sub> concentration) to normalize the response and to validate GluCl  
21 346 expression. An extra two min non-recorded wash-out was maintained between  
22 347 abamectin applications to further allow the current to return to baseline as  
23 348 desensitization from abamectin is slow. Next, abamectin was co-applied with L-  
24 349 glutamic acid for 30 sec to both wild type and I321T injected oocytes to test abamectin  
25 350 potentiation of glutamate-induced currents. Responses to L-glutamic acid applications  
26 351 were normalized ( $I\% = (I / I_{max}) \times 100$ ) and graphed as means  $\pm$  SEM (standard error  
27 352 of the mean) using at least 6 oocytes. TEVC recordings were analyzed using the  
28 353 Roboocyte 2+ V. 1.4.3. software (Multi Channel Systems MCS GmbH), EC<sub>50</sub>, pEC<sub>50</sub>  
29 354 values and Hill coefficients were calculated by fitting a four-parameter logistic curve  
30 355 (Hill equation) on response data using SigmaPlot software 13.0 (Systat Software, San  
31 356 Jose, CA, USA).

### 32 357 **2.6.4 Actions of $\gamma$ -aminobutyric acid and abamectin on wild type *T. urticae* Rdl3**

33 358 The activity of  $\gamma$ -aminobutyric acid (GABA; CAS number 56-12-2; Sigma–Aldrich) and  
34 359 abamectin on three *T. urticae* Rdl3 (Rdl1, Rdl2 or Rdl3) channels was examined as  
35 360 described above, with a prolonged abamectin application of 3 min. To assess the  
36 361 antagonistic effect of abamectin, oocytes were tested based on Rufener *et al.* 2017.<sup>59</sup>  
37 362 Oocytes were first exposed to GABA (EC<sub>5</sub>, EC<sub>50</sub> or EC<sub>90</sub> concentration) 4 times for 30  
38 363 s every 1.5 min at the beginning of the experiment to test for Rdl expression and to

1  
2  
3 364 stabilize the response. Subsequently, oocytes were pre-exposed for 75 s to abamectin  
4 365 (1 nM-10  $\mu$ M) followed by 30 s of co-applied GABA ( $EC_{50}$ ) and abamectin. Both  
5 366 compounds were washed out (non-recorded) for 3.5 min before increasing to the next  
6 367 concentration.

## 11 368 **2.7 Figure editing**

12 369 CorelDRAW Home & Student  $\times 7$ , SigmaPlot 13.0 and GraphPad Prism 5 software  
13 370 were used to process and edit the figures.

## 16 371 **3 RESULTS**

### 19 372 **3.1 Genotyping of GluCl TM3 and Rdl TM2/TM3 regions in *T. urticae* field** 20 373 **isolates**

21 374 During a target-site (GluCl) screening of 32 European field *T. urticae* strains, we  
22 375 previously detected an I321T (ATT->ACT) mutation in GluCl3 in four abamectin  
23 376 resistant strains from Spain and Italy (Fig. S4 and Table S2).<sup>36</sup> To further explore the  
24 377 occurrence of this mutation in Europe, a number of additional strains were tested which  
25 378 revealed the occurrence of the mutation in a abamectin resistant field strain from  
26 379 Turkey (TR2) and a multi-acaricide resistant strain from Belgium, MR-VL<sup>46</sup> (Fig. S4 and  
27 380 Table S2). The mutation I321T was fixed in MR-VL but was segregating in TR2. PCR  
28 381 and sequencing confirmed the absence of TM3 mutations in all five GluCl genes in the  
29 382 susceptible strain SR6. As Rdl is considered as a potential secondary target of  
30 383 macrocyclic lactones,<sup>12,27,28</sup> the TM2/TM3 fragments of three Rdl genes were also  
31 384 screened for all seven strains in this study but no mutations were identified [in any of](#)  
32 385 [the tested strains.](#)

### 34 386 **3.2 Abamectin resistance levels**

35 387 [The results of the toxicity tests are listed in Table S2. The strains IT1, IT5, IT6 and TR2](#)  
36 388 [with only the I321T mutation in TM3 region of GluCl3, were all resistant to abamectin](#)  
37 389 [with  \$LC\_{50}\$ s over 10 mg a.i./L and resistance ratios \(RRs\) ranging from 46.63- to 104.0-](#)  
38 390 [fold compared to the susceptible strain SR6. The ES1 strain with three segregating](#)  
39 391 [mutations I321T/V327G/L329F in GluCl3 showed the highest levels of abamectin](#)  
40 392 [resistance \(78.59 mg a.i. /L\) with RRs reaching 327.5 -fold. Another strain MR-VL \(with](#)  
41 393 [the I321T mutation in TM3 region of GluCl3\) exhibited low levels of abamectin](#)  
42 394 [resistance \(1.79 mg a.i. /L\) with only 7.46-fold RR.](#)

### 395 **3.3 Backcrossing experiments**

#### 396 **3.3.1 Establishment of congenic lines**

397 Two backcross experiments (BC1 and BC2) were carried out between a parental  
398 resistant strain, fixed for the I321T GluCl3 mutation, and a susceptible strain, lacking  
399 the mutation (BC1: ♀ SR6 x ♂ TR2 and BC2: ♀ SR6 x ♂ IT6). After seven rounds of  
400 backcrossing and the final cross between heterozygous backcrossed females and their  
401 sons, two lines that were homozygous for the I321T mutation (TRA\_R1, TRA\_R2;  
402 T321/T321 genotype), and two congenic control lines, lacking the mutation (TRA\_C1,  
403 TRA\_C2; I321/I321 genotype), were obtained for BC1. For the BC2 experiment, three  
404 lines with the T321/T321 genotype (ITA\_R1, ITA\_R2, ITA\_R3) and three susceptible  
405 control lines with the I321/I321 genotype (ITA\_C1, ITA\_C2, ITA\_C3) were obtained.

#### 406 **3.3.2 Toxicity assays of congenic lines**

407 Before the start of the backcross experiments, abamectin was tested on all parental  
408 strains (SR6, TR2 and IT6). The abamectin RR of TR2 and IT6 was 82 and 105 -fold  
409 respectively (Table 1). In BC1, the lines with the T321/T321 genotype showed  
410 resistance to abamectin with RRs up to 50-fold (Table 1) while for BC2, RRs of the  
411 lines with the T321/T321 genotype were less than two-fold and not significantly  
412 different from 1 (Table 1).

### 413 **3.4 CRISPR-Cas9 genome editing in *Drosophila***

#### 414 **3.4.1 Introduction of I321T in *Drosophila* GluCl**

415 Several genome-edited fly lines bearing an I321T (*T. urticae* GluCl3 numbering)  
416 mutation in the GluCl gene were established. We confirmed the presence of HDR-  
417 derived alleles in five out of eighteen different G<sub>0</sub> lines that gave G<sub>1</sub> progeny (Fig. S3).  
418 Two phenotypically homozygous lines were sequence verified, bearing the correct  
419 mutation (Fig. S3c) at the *Drosophila* GluCl gene. One of these was used for  
420 downstream toxicity bioassays. Feeding toxicity bioassays with *Drosophila* larvae  
421 against abamectin were carried out using nos.Cas9 flies as controls. *Drosophila* larvae  
422 were in continuous contact with the insecticide containing food. Since the fly larvae are  
423 not readily visible in the food, we considered pupation efficiency as a measurable proxy  
424 of eventual survival. The results (Table 2) indicate that flies bearing the I321T mutation  
425 are more resistant to abamectin than the control (nos.Cas9) flies carrying the wild-type  
426 *Drosophila* GluCl allelic combination. As shown in Table 2, LC<sub>50</sub> value for nos.Cas9 is

1  
2  
3 427 0.018 mg/L (95% CI: 0.014 - 0.020), while for I321T flies the corresponding value is  
4  
5 428 0.048 mg/L (95% CI: 0.039 - 0.055), which translates to a resistance ratio (RR) of 2.7  
6  
7 429 folds. It must be noted, however, that I321T flies apparently exhibited slower  
8  
9 430 development when exposed to abamectin, even at the lowest concentration (c. 15 days  
10  
11 431 from egg to adult at 25°C compared to 10-11 days for the nos.Cas9 background strain)

### 12 432 **3.4.2 Introduction of G314D or G326E in *Drosophila* GluCI**

13  
14 433 Several genome-edited fly lines bearing the G314D or G326E mutation (*T. urticae*  
15  
16 434 GluCI1 and GluCI3 numbering, respectively) in the GluCI gene were generated. The  
17  
18 435 presence of HDR-derived alleles in ten out of thirty-nine different G<sub>0</sub> lines that gave G<sub>1</sub>  
19  
20 436 progeny for G314D and seven out of seventeen G<sub>0</sub> lines for G326E was confirmed.  
21  
22 437 Several independent lines were established and balanced, but at the final crossing  
23  
24 438 step virtually no phenotypically homozygous flies could be identified, indicating an  
25  
26 439 associated lethality in both genome-modified alleles. A very small number of “escaper”  
27  
28 440 flies without the balancer-associated marker *Stubble* was eventually observed after  
29  
30 441 several generations of inter-crosses between heterozygotes derived from the same or  
31  
32 442 different G<sub>0</sub> lines (three flies in total among several thousands of screened progeny).  
33  
34 443 These flies were all male, much smaller than their heterozygous siblings and when  
35  
36 444 crosses were attempted, all three were sterile and only survived for a few days. In order  
37  
38 445 to further investigate the G314D/G326E associated lethality, a complementation  
39  
40 446 experiment was performed by crossing heterozygous G314D/TM3 or G326E/TM3 flies  
41  
42 447 with strain #25726 from Bloomington *Drosophila* stock centre (genotype w[1118];  
43  
44 448 Df(3R)BSC636/TM6C, cu[1] Sb[1]) which carries a chromosomal deletion at  
45  
46 449 chromosome 3R at a region that includes the GluCI $\alpha$  gene of *Drosophila*. These  
47  
48 450 crosses never produced any progeny not bearing the parental balancer chromosomes,  
49  
50 451 indicating that indeed the lethality is linked to the deleted region that contains GluCI $\alpha$ .  
51  
52 452 Taken together, these observations suggest it is highly likely that both G314D and  
53  
54 453 G326E are essentially lethal, i.e. have severe impact on channel function and viability.

### 51 454 **3.5 Two-electrode voltage-clamp electrophysiology**

#### 53 455 **3.5.1 Responses of *T. urticae* GluCI3 WT and GluCI3 I321T to L-glutamic acid** 55 456 **and abamectin**

57 457 Two homomeric GluCI channels, consisting either solely of GluCI3 wild type (WT)  
58  
59 458 subunits or GluCI3 I321T subunits, were expressed in *Xenopus* oocytes and the  
60

1  
2  
3 459 responsiveness of these channels was examined for L-glutamic acid and abamectin.  
4  
5 460 As previously described in Mermans et al. 2017, GluCl3 WT channels generate robust  
6  
7 461 responses to L-glutamic acid with rapid inward currents and fast desensitization.<sup>38</sup> In  
8  
9 462 contrast, only few of the GluCl3 I321T injected oocytes showed clear responses to L-  
10  
11 463 glutamic acid, with generally smaller amplitudes of currents but with the same response  
12  
13 464 profile as GluCl3 WT indicating that only in a fraction of the oocytes functional GluCl3  
14  
15 465 I321T receptors were formed (Fig. 2a). L-glutamic acid dose-response curves resulted  
16  
17 466 in EC<sub>50</sub>s of 476.4 μM (pEC<sub>50</sub> = 3.32 ± 0.01) and 311.3 μM (pEC<sub>50</sub>=3.51 ± 0.02) and Hill  
18  
19 467 coefficients of 2.34 ± 0.14 and 2.42 ± 0.31 for GluCl3 WT and GluCl3 I321T  
20  
21 468 respectively (Fig. 2d, Table 3).

22  
23 469 Next, to investigate whether both channels were activated by abamectin,  
24  
25 470 injected oocytes were first tested for expression through application of EC<sub>50</sub> L-glutamic  
26  
27 471 acid. When clear inward currents were observed, the oocytes were subjected to an  
28  
29 472 increasing concentration of abamectin (1 nM - 100 μM) with an extensive wash of 3.5  
30  
31 473 min in between every concentration. Abamectin elicited inward currents through  
32  
33 474 GluCl3 WT channels with a slow onset and a very slow desensitization in comparison  
34  
35 475 to L-glutamic acid responses. The same was observed for oocytes expressing GluCl3  
36  
37 476 I321T, but again with a significantly (around 10-fold) smaller amplitude of currents  
38  
39 477 compared to GluCl3 WT (Fig. 2b). While GluCl3 WT channels showed a clear dose  
40  
41 478 dependent response, GluCl3 I321T channels seemed more insensitive to the increase  
42  
43 479 of concentrations of abamectin (Fig. 2c). Therefore, an unambiguous abamectin EC<sub>50</sub>  
44  
45 480 could only be calculated for GluCl3 WT (EC<sub>50</sub> =447 nM (pEC<sub>50</sub> = 6.32 ± 0.12)). No  
46  
47 481 responses to L-glutamic acid and abamectin were observed in any oocyte injected with  
48  
49 482 water alone (data not shown).

50  
51 483 Subsequently, abamectin potentiation of L-glutamic induced currents was  
52  
53 484 examined in both GluCl3 channels by perfusion with 1 mM of L-glutamic acid followed  
54  
55 485 by co-application of 1 mM L-glutamic acid and 100 nM abamectin. The amplitude of  
56  
57 486 currents induced by the L-glutamic acid was increased by the perfusion of abamectin  
58  
59 487 in wild-type GluCl3. In contrast, no clear potentiation of glutamate-induced currents  
60  
488 was observed in oocytes expressing GluCl3 I321T (Fig. 2c). GluCl3 G326E was tested  
489 again in this study and, as in our previous study, GluCl3 G326E was not activated by  
490 abamectin even when tested at high concentrations nor could abamectin potentiate  
491 the L-glutamic acid response when co-applied (Fig. 2b&c).<sup>38</sup>



### 3.5.2 Responses of *T. urticae* Rdl1 to GABA and abamectin

All three channels showed robust responses to the natural agonist GABA, generating rapid inward currents with a slow desensitization as long as the agonist was applied, followed by a very rapid desensitization once wash-out with NFR was started. The averaged dose-response curves for GABA were characterized by an EC<sub>50</sub> of 15.45 μM (pEC<sub>50</sub>= 4.8 ± 0.007), 68.6 μM (pEC<sub>50</sub>=4.16 ± 0.034) and 139.8 μM (pEC<sub>50</sub>=3.85 ± 0.035) for Rdl1, Rdl2 and Rdl3 respectively (Fig. 3c and Table 4). To assess the agonistic effect of abamectin, the compound was first applied alone to Rdl1, Rdl2 or Rdl3 expressed in oocytes for 3min, but the channels were not activated by abamectin (Fig. 3a). Although, when tested at high concentrations (10-100 μM), abamectin elicited very small inward currents which are negligible in amplitude compared to the GABA response (Fig. S6). To test antagonistic properties of abamectin, a cumulative exposure was used where the oocytes were pre-incubated with abamectin for 75 s followed by co-application of abamectin and GABA to ensure the maximum inhibitory effect. Perfusion of abamectin produced a dose-dependent inhibition of the GABA response for Rdl1, Rdl2 and Rdl3 regardless when EC<sub>5</sub>, EC<sub>50</sub> or EC<sub>90</sub> of GABA was applied (Fig. 3b-d, Fig. S5 and Table 4).

## 4 DISCUSSION

Abamectin has been used extensively for spider mite control, and over the years various levels of abamectin resistance have been detected in *T. urticae* populations worldwide.<sup>31,33,36,45,60</sup> The molecular mechanism underlying abamectin resistance in *T. urticae* have been investigated in a number of strains and both enhanced metabolic detoxification as well as target-site resistance mutations were shown to be at play. In particular, gene-expression analysis and functional characterization have pointed towards the involvement of cytochrome P450s (P450s), glutathione-S-transferases (GSTs) and uridine diphosphate (UDP) - glycosyltransferases (UGTs).<sup>36,61,62</sup> In addition, two mutations, G314D in *GluCl1* and G326E in *GluCl3*, were shown to be genetically linked to abamectin resistance and both G314D and G326E have been functionally validated by two-electrode voltage-clamp electrophysiology in *Xenopus*.<sup>14,37-40</sup> Intriguingly, in contrast to the electrophysiological validation, introgression of mutations in GluCl1 in a susceptible background have revealed only a relatively weak resistance phenotype. It is therefore clear that the interplay between different receptors, their mutations and potential synergistic actions of additional

1  
2  
3 525 mechanisms of resistance, is far from completely understood, and in part also the  
4  
5 526 objective of this study.

6 527 Recently, abamectin and milbemectin (cross)-resistance mechanisms have  
7  
8 528 been studied in an exceptionally wide collection of strains sampled across Europe.  
9  
10 529 Aside from confirming the presence of both increased detoxification and previously  
11  
12 530 described target-site mutations, this study also uncovered the presence of a potential  
13  
14 531 new target-site mutation, I321T in GluCl3. Surprisingly, this mutation was only found  
15  
16 532 in populations consisting of the red color morph of *T. urticae*.<sup>36</sup> We further confirm in  
17  
18 533 this study the presence of this mutation in two additional red *T. urticae* strains, TR2  
19  
20 534 and MR-VL from Turkey and Belgium, respectively<sup>45,46</sup> (Table S2) and recently, it was  
21  
22 535 also detected in a Greek multi-resistant red spider mite population.<sup>41</sup> Based on receptor  
23  
24 536 sequences of green and red color morphs (Fig. S4), phylogenetic constraints do not  
25  
26 537 seem to explain why this mutation only occurs in red morphs, and given the  
27  
28 538 geographical origin of the strains under investigation, a single origin and spread of the  
29  
30 539 mutation does not seem likely, although it is impossible to exclude.

31 540 The potential relevance of I321T in abamectin resistance can first be inferred  
32  
33 541 from its location in TM3, which is at the periphery of the predicted glutamate binding  
34  
35 542 site and was previously reported to be involved in ivermectin binding, based on the  
36  
37 543 GluCl $\alpha$  crystal structure of *C. elegans*.<sup>7</sup> In addition, an A309V mutation in *P. xylostella*  
38  
39 544 GluCl, adjacent to I321 in *T. urticae* GluCl3, was also strongly associated with  
40  
41 545 abamectin resistance (Fig. 1a&b).<sup>39,63</sup>

42 546 We used the *Xenopus* system to investigate the role of the I321T mutation in  
43  
44 547 the interaction of abamectin with GluCl. Compared to GluCl3 WT, functional GluCl3  
45  
46 548 I321T was only successfully expressed in a limited number of oocytes, and L-glutamic  
47  
48 549 acid induced currents had a significantly lower amplitude in these channels. The lack  
49  
50 550 of GluCl3 I321T expression could either be due to a reduced translation of the  
51  
52 551 exogenous cRNA in *Xenopus* oocytes or it is possible that only few of the formed  
53  
54 552 receptors are functional i.e. that binding of ligands and ivermectin is compromised or  
55  
56 553 that the ion channel is unable to open to its normal extend. Either way, the GluCl3  
57  
58 554 I321T mutation seems to influence GluCl3 I321T expression as both GluCl3 WT and  
59  
60 555 G326E showed consistent expression in *Xenopus* oocytes when established with the  
61  
62 556 same protocol.<sup>38</sup>

63 557 Nevertheless, L-glutamic acid dose-response curves could be calculated for  
64  
65 558 both GluCl3 WT and GluCl3 I321T channels, and the L-glutamic acid EC<sub>50</sub> for both

1  
2  
3 559 channels differed by 1.5 fold (Table 3) only, which is in line with previous studies that  
4 560 examined the effect of GluCl resistance mutations using *Xenopus*.<sup>38,39</sup> For both GluCl3  
5 561 WT and GluCl3 I321T abamectin induced currents could be observed, but, as with L-  
6 562 glutamic acid induced currents, the amplitude of response was significantly lower for  
7 563 GluCl3 I321T. Further, no clear potentiation of glutamate-induced currents was  
8 564 observed after co-application of 1 mM L-glutamic acid and 100 nM abamectin in GluCl3  
9 565 I321T expressing oocytes while such increase was observed for GluCl3 WT. This  
10 566 subtle effect of the I321T mutation on abamectin response is in contrast to the G314D  
11 567 and G326E mutation, which completely abolished the agonist activity of abamectin and  
12 568 milbemycin A<sub>4</sub>, another macrocyclic lactone (Fig. 2b).<sup>38</sup> But in line with the study of  
13 569 Wang et al., the A309V mutation in *P. xylostella* GluCl (corresponding to A320 and  
14 570 located next to I321 in *T. urticae* GluCl3) only resulted in 4.8 fold reduced sensitivity,  
15 571 while the G315E mutation (corresponding to G326E in *T. urticae* GluCl3) reduced the  
16 572 sensitivity to abamectin by 493-fold.<sup>39</sup> This difference in effect might be explained by  
17 573 the interaction of these residues with macrocyclic lactones. Based on the crystal  
18 574 structure of *C. elegans* GluCl $\alpha$  and its predicted binding to ivermectin, A320 and I321  
19 575 are not predicted to interact with ivermectin while G326E is predicted to have van der  
20 576 Waals interactions with ivermectin and is located closest to ivermectin (Fig. 1b).<sup>7</sup>  
21 577 However, Wang et al. 2017, predicted that *P. xylostella* GluCl A309V mutants might  
22 578 allosterically offset the functional effect of abamectin upon binding,<sup>39</sup> and our findings  
23 579 suggest that this prediction also holds for the GluCl3 I321T mutation, with I321T having  
24 580 an effect on abamectin action, much likely by reducing channel sensitivity.

25 581 To further corroborate the possible likelihood of this mutation to be involved in  
26 582 abamectin resistance, the relative phenotypic contribution of the I321T mutation was  
27 583 first characterized by marker-assisted backcrossing. Two independent backcrossing  
28 584 experiments (BC1 and BC2) originating from two genetically different strains from  
29 585 distinct geographical origin were performed. Each experiment resulted in congenic  
30 586 lines, either homozygous for the mutant (T321/T321) or wildtype (I321/I321) GluCl3  
31 587 allele. For BC1, resistance ratios reached over 50-fold (Table 1) compared to the  
32 588 wildtype lines, but in contrast, for BC2 only low levels of abamectin resistance were  
33 589 observed in the mutant lines. The result of BC2 is similar to Riga et al. 2017, where  
34 590 only low levels of resistance were observed when either G314D in GluCl1 or G326E in  
35 591 GluCl3 was introgressed, indicating that a mutation in GluCl1 and GluCl3 alone was  
36 592 insufficient to convey resistance.<sup>51</sup>

1  
2  
3 593 Marker-assisted back-crossing is expected to uncouple multiple resistance  
4 594 factors and reduces the proportion of donor genome with every cycle. However, if  
5 595 resistance genes are closely located together on the chromosome, chances to capture  
6 596 recombination events between adjacent genes are rare. Hence, to explain the variance  
7 597 between the mutant congenic lines of BC1 and BC2, one could argue that in BC1 the  
8 598 uncoupling of resistance genes might not have succeeded because of linkage. The  
9 599 fact that the mutation alone does not convey high resistance levels was also clear from  
10 600 the laboratory reference resistant strain MR-VL. Although this strain was fixed for the  
11 601 mutation, it is not highly resistant to abamectin (Table 1). Since this strain has not been  
12 602 selected with abamectin for more than ten years, additional factors that might  
13 603 contribute to resistance were probably lost, mimicking the effect of introgression. What  
14 604 these extra resistance factors might be is hard to resolve and could be any regulatory  
15 605 element of a detoxification enzyme or factors resulting in compositional changes of  
16 606 GluCl channels (i.e. overexpression/ underexpression of certain GluCl genes).

17 607 Indeed, the differences between BC1 and BC2 and low resistance levels of MR-  
18 608 VL point towards a lack of understanding of the role of mutations in resistance that was  
19 609 already previously clear from introgression work with other mutations in GluCl1 and  
20 610 GluCl3. These mutations also provide a weak phenotype *in vivo*, despite the complete  
21 611 lack of agonistic activity in electrophysiological studies.<sup>40</sup> The complexity of the channel  
22 612 confirmation might be one of the factors involved. For example, a GluCl channel could  
23 613 consist of five GluCl3 encoded subunits, each carrying the I321T mutation (homomeric  
24 614 GluCl channel), or could be composed of GluCl subunits with or without mutation  
25 615 (heteromeric GluCl channel with subunits encoded by different genes) (Fig. 1c); the  
26 616 latter channel being likely more sensitive to abamectin. Alternatively, less-sensitive  
27 617 abamectin receptors could be formed through combination of GluCl and non-GluCl  
28 618 subunits.<sup>12</sup> In Xue et al. 2020, it was shown that two cys-loop ligand gated ion channel  
29 619 subunit genes (*tetur02g11020* and *tetur02g11170*), were overexpressed in abamectin  
30 620 resistant strains. The *Drosophila* ortholog (CG12344) of these genes has only been  
31 621 poorly characterized but encode subunits of a cys-loop LGIC predicted to be most  
32 622 related to vertebrate glycine receptors (<http://flybase.org/reports/FBgn0033558.html>).  
33 623 Interestingly, vertebrate glycine receptors are 100-fold less sensitive to ivermectin  
34 624 compared to invertebrate GluClS as they lack the TM3 glycine residue at a position  
35 625 corresponding to G314/G326 in *T. urticae* GluCl1/GluCl3<sup>14,64,65</sup> and hence heteromeric  
36 626 cys-loop channels consisting of *GluCl* and *tetur02g11020/tetur02g11170* encoded

1  
2  
3 627 subunits might be less sensitive to abamectin. Alternatively, less-sensitive abamectin  
4 628 receptors might also consist of a mix of GluCl and Rdl subunits (Fig. 1c). Such  
5 629 channels have been reported before,<sup>12</sup> and homomeric Rdl channels were reported to  
6 630 be more than 150-fold less sensitive to ivermectin compared to GluCl channels.<sup>26</sup>

7  
8  
9  
10 631 Therefore, to infer whether abamectin also acts on *T. urticae* Rdl channels, three  
11 632 homomeric *T. urticae* Rdl channels,<sup>14</sup> consisting either of *T. urticae Rdl1*, *Rdl2* or *Rdl3*  
12 633 (encoded subunits) were expressed using *Xenopus* oocytes. Abamectin alone did not  
13 634 invoke Rdl currents but had an antagonistic effect on all three *T. urticae* Rdl channels  
14 635 (Fig. 3 and Table 4). These observations are in line with Xu et al. 2017, in which  
15 636 *Tetranychus* Rdl channels were not activated by abamectin or ivermectin alone.  
16 637 However, a follow-up study of the same group showed that abamectin has an agonistic  
17 638 action on *Tetranychus* Rdl2.<sup>66,67</sup> On the other hand, for insect and nematode Rdl, the  
18 639 action of ivermectin was shown to be dependent on application conditions<sup>26,68</sup> and our  
19 640 results are in agreement with previous electrophysiology studies showing that  
20 641 application of ivermectin alone does not have any effect on the receptor<sup>69,70</sup> and reports  
21 642 showing that ivermectin is an antagonist of GABA induced Rdl currents at a GABA  
22 643 concentration higher than the EC<sub>50</sub>.<sup>26,68,69</sup> This suggests that indeed, to survive high  
23 644 concentration of abamectin, a detoxification component or additional factor is needed  
24 645 to protect against additional Rdl interactions.

25  
26  
27  
28  
29  
30  
31  
32  
33  
34  
35  
36 646 As there was no conclusive outcome from the backcrossing experiments, we  
37 647 next used the CRISPR-Cas9 technology to introduce the I321T mutation in the GluCl  
38 648 homologue of *D. melanogaster*. In the past, this technology was shown to be a very  
39 649 useful tool to elucidate the role of a single amino acid substitution in resistance against  
40 650 insecticides.<sup>71</sup> Two phenotypically homozygous fly lines bearing an I321T mutation in  
41 651 *GluCl* were generated. Toxicity bioassays with one of these lines revealed moderate  
42 652 abamectin resistance levels in the *GluCl* I321T line compared to the control. In addition,  
43 653 we also observed a fitness-cost (although we did not quantify) in the *GluCl* I321T line,  
44 654 with developmental time being much slower in I321T flies exposed to abamectin  
45 655 compared to control flies. To better interpret the effects of the *GluCl* I321T mutation in  
46 656 *Drosophila*, we also tried to introduce the previously documented abamectin resistance  
47 657 mutations, G314D in *GluCl1* and G326E in *GluCl3*, in *Drosophila* GluCl. Unfortunately,  
48 658 no phenotypically homozygous flies could be identified at the final crossing step, and  
49 659 crosses between heterozygous G314D/TM3 or G326E/TM3 flies and a fly strain that  
50 660 had a chromosomal deletion in the GluCl $\alpha$  region, yielded no viable progeny; strongly

1  
2  
3 661 suggesting these mutations cause lethality. A lethal phenotype for flies with CRISPRed  
4 662 resistance mutation(s) has been reported before; see for example Bajda et al. 2017,  
5 663 Douris et al 2017 or Douris et al, 2020.<sup>55,71,72</sup> Hence, *Drosophila* is not always a suitable  
6 664 species for reverse genetics with resistance mutations that were detected in other  
7 665 species. In the case of *T. urticae* and abamectin resistance, this is further complicated  
8 666 by the fact that there is only one *GluCl* gene in *Drosophila* while there are at least five  
9 667 in *T. urticae*.<sup>14,17</sup>

15 668 Hence, ideally, one would introduce the *GluCl* mutations in *T. urticae*. As it was  
16 669 recently shown that CRISPR-Cas9 can be used to create gene knockouts in *T.*  
17 670 *urticae*,<sup>73</sup> this type of gene-editing might soon be a feasible genetic tool for this species.  
18 671 Nevertheless, the lethality of the G314D/G326E mutations in *Drosophila* does imply  
19 672 that these residues have an important role in channel functioning, and is in line with a  
20 673 previously documented fitness cost of G314D and G326E in *T. urticae*.<sup>74</sup>

## 26 674 5 CONCLUSION

27 675 To conclude, the role of the *GluCl3* I321T mutation in abamectin resistance of *T. urticae*  
28 676 was examined by *in vitro* functional expression and electrophysiology, backcrossing  
29 677 experiments and CRISPR-Cas9 gene editing in *Drosophila*. Based on backcross  
30 678 experiments, the I321T mutation alone did not always result in high abamectin  
31 679 resistance levels, a finding also reported for other mutations in *GluCl1* and *GluCl3*.  
32 680 Genome editing in *Drosophila* confirmed the role of *GluCl3* I321T in resistance, but  
33 681 again with low resistance levels. Functional analysis using *Xenopus* oocytes showed  
34 682 that the I321T mutation could reduce *GluCl* sensitivity to abamectin, but whether this  
35 683 reduction is actually due to the effect of the I321T mutation or resulting from decreased  
36 684 expression remains unclear. We confirm the antagonistic effect of abamectin on all  
37 685 three Rdl, suggesting that abamectin also acts on Rdl at high doses in *T. urticae*.  
38 686 We therefore propose that the I321T *GluCl3* mutation plays a role in abamectin  
39 687 resistance, but only in combination with synergistic additional factors that deserve  
40 688 more investigation.<sup>75</sup>

## 52 689 6 ACKNOWLEDGEMENTS

53 690 We would like to thank professor Christos Delidakis (Institute of Molecular Biology and  
54 691 Biotechnology (IMBB)/University of Crete, Greece) for providing the balancer stock  
55 692 TM3/ TM6B, Maria Riga and Evangelia Skoufa (IMBB/University of Crete) for their help  
56 693 with *Drosophila* toxicity bioassays and Brian Gratwicke for a photograph of *Xenopus*

1  
2  
3 694 *laevis* (graphical abstract). Wenxin Xue is the recipient of a doctoral grant from China  
4  
5 695 Scholarship Council (CSC) and co-funded by Ghent University BOF-UGent (from  
6  
7 696 03/2017 to 07/2019). This work was supported by the European Union's Horizon 2020  
8  
9 697 research and innovation program [ERC consolidator grant 772026-POLYADAPT to  
10  
11 698 TVL and 773902-SuperPests to TVL and JV].

## 12 699 **7 SUPPORTING INFORMATION**

13  
14 700 Supporting information might be found in the online version of this article.

## 15 16 701 **8 REFERENCES**

- 17  
18 702 1 Hallock KF, Sutter M, Gneezy U, Grossman PJ, Results E, Plott CR, *et al.*,  
19  
20 703 Surviving in a Toxic World, 545–547 (2012).
- 21 704 2 Wolstenholme AJ and Rogers AT, Glutamate-gated chloride channels and the  
22  
23 705 mode of action of the avermectin/milbemycin anthelmintics, *Parasitology* **131**  
24  
25 706 (2005).
- 26 707 3 Shoop WL, Mrozik H and Fisher MH, Structure and activity of avermectins and  
27  
28 708 milbemycins in animal health, *Vet Parasitol* **59**:139–156 (1995).
- 29  
30 709 4 Burg RW, Miller BM, Baker EE, Birnbaum J, Currie SA, Hartman R, *et al.*,  
31  
32 710 Avermectins, new family of potent anthelmintic agents: Producing organism and  
33  
34 711 fermentation, *Antimicrob Agents Chemother* **15**:361–367 (1979).
- 35 712 5 Pitterna T., Chloride channel activators/new natural products: avermectins and  
36  
37 713 milbemycins, *Mod Crop Prot Compd*, ed. by Wolfgang Kramer, Ulrich Schirmer,  
38  
39 714 Peter Jeschke MW (2011).
- 40 715 6 Horenstein J, Wagner DA, Czajkowski C and Akabas MH, Protein mobility and  
41  
42 716 GABA-induced conformational changes in GABA A receptor pore-lining M2  
43  
44 717 segment, *Nat Neurosci* **4**:447–485 (2001).
- 45 718 7 Hibbs RE and Gouaux E, Principles of activation and permeation in an anion-  
46  
47 719 selective Cys-loop receptor, *Nature* **474**:54–60 (2011).
- 48  
49 720 8 Ghosh R, Andersen EC, Shapiro J a, Gerke JP and Kruglyak L, Natural Variation  
50  
51 721 in a Chloride Channel Subunit Confers Avermectin Resistance in *C. elegans*,  
52  
53 722 *Science (80- )* **335**:574–578 (2012).
- 54 723 9 Ozoe Y, g -Aminobutyrate- and Glutamate-gated Chloride Channels as Targets  
55  
56 724 of Insecticides, 1st ed., *Target Recept Control Insect Pests* **44**, 1st ed., Elsevier  
57  
58 725 Ltd. (2013).
- 59 726 10 Castle SJ, Merten P and Prabhaker N, Comparative susceptibility of Bemisia

- 1  
2  
3 727 tabaci to imidacloprid in field- and laboratory-based bioassays, *Pest Manag Sci*  
4 728 **70**:1538–1546 (2014).  
5  
6 729 11 Prichard R, Ménez C and Lespine A, Moxidectin and the avermectins:  
7 730 Consanguinity but not identity, *Int J Parasitol Drugs Drug Resist* **2**:134–153,  
8 731 Australian Society for Parasitology (2012).  
9  
10 732 12 Ludmerer SW, Warren VA, Williams BS, Zheng Y, Hunt DC, Ayer MB, *et al.*,  
11 733 Ivermectin and nodulisporic acid receptors in *Drosophila melanogaster* contain  
12 734 both  $\gamma$ -aminobutyric acid-gated Rdl and glutamate-gated GluCl $\alpha$  chloride  
13 735 channel subunits, *Biochemistry* **41**:6548–6560 (2002).  
14  
15 736 13 Clark JM, Scott JG, Campos F and Bloomquist JR, Resistance to Avermectins:  
16 737 Extent, Mechanisms, and Management Implications, *Annu Rev Entomol* **40**:1–  
17 738 30 (1995).  
18  
19 739 14 Dermauw W, Ilias A, Riga M, Tsagkarakou A, Grbić M, Tirry L, *et al.*, The cys-  
20 740 loop ligand-gated ion channel gene family of *Tetranychus urticae*: Implications  
21 741 for acaricide toxicology and a novel mutation associated with abamectin  
22 742 resistance, *Insect Biochem Mol Biol* **42**:455–465 (2012).  
23  
24 743 15 Cully DF, Vassilatis DK, Liu KK, Paress PS, Van der Ploeg LHT, Schaeffer JM,  
25 744 *et al.*, Cloning of an avermectin-sensitive glutamate-gated chloride channel from  
26 745 *Caenorhabditis elegans*, *Nature* **371**:707–711 (1994).  
27  
28 746 16 Brown DDR, Siddiqui SZ, Kaji MD and Forrester SG, Pharmacological  
29 747 characterization of the *Haemonchus contortus* GABA-gated chloride channel,  
30 748 Hco-UNC-49: Modulation by macrocyclic lactone anthelmintics and a receptor  
31 749 for piperazine, *Vet Parasitol* **185**:201–209, Elsevier B.V. (2012).  
32  
33 750 17 Knipple DC and Soderlund DM, The ligand-gated chloride channel gene family  
34 751 of *Drosophila melanogaster*, *Pestic Biochem Physiol* **97**:140–148, Elsevier Inc.  
35 752 (2010).  
36  
37 753 18 Jones AK, Bera AN, Lees K and Sattelle DB, The cys-loop ligand-gated ion  
38 754 channel gene superfamily of the parasitoid wasp, *Nasonia vitripennis*, *Heredity*  
39 755 (*Edinb*) **104**:247–259, Nature Publishing Group (2010).  
40  
41 756 19 Jones AK and Sattelle DB, The cys-loop ligand-gated ion channel gene  
42 757 superfamily of the red flour beetle, *tribolium castaneum*, *BMC Genomics* **8**:1–16  
43 758 (2007).  
44  
45 759 20 Jones AK and Sattelle DB, The cys-loop ligand-gated ion channel superfamily of  
46 760 the honeybee, *Apis mellifera*, *Invertebr Neurosci* **6**:123–132 (2006).



- 1  
2  
3 761 21 Ménard C, Folacci M, Brunello L, Charreton M, Collet C, Mary R, *et al.*, Multiple  
4 762 combinations of RDL subunits diversify the repertoire of GABA receptors in the  
5 763 honey bee parasite *Varroa destructor*, *J Biol Chem* **293**:19012–19024 (2018).  
6  
7  
8 764 22 Kehoe J, Buldakova S, Acher F, Dent J, Bregestovski P and Bradley J, Aplysia  
9 765 cys-loop glutamate-gated chloride channels reveal convergent evolution of  
10 766 ligand specificity, *J Mol Evol* **69**:125–141 (2009).  
11  
12  
13 767 23 Beech R, Levitt N, Cambos M, Zhou S and Forrester SG, Association of ion-  
14 768 channel genotype and macrocyclic lactone sensitivity traits in *Haemonchus*  
15 769 *contortus*, *Mol Biochem Parasitol* **171**:74–80, Elsevier B.V. (2010).  
16  
17  
18 770 24 Wolstenholme AJ, Glutamate-gated chloride channels, *J Biol Chem* **287**:40232–  
19 771 40238 (2012).  
20  
21  
22 772 25 Sparks TC and Nauen R, IRAC: Mode of action classification and insecticide  
23 773 resistance management, *Pestic Biochem Physiol* **121**:122–128, The Authors  
24 774 (2015).  
25  
26  
27 775 26 Fuse T, Kita T, Nakata Y, Ozoe F and Ozoe Y, Electrophysiological  
28 776 characterization of ivermectin triple actions on *Musca* chloride channels gated  
29 777 by L-glutamic acid and  $\gamma$ -aminobutyric acid, *Insect Biochem Mol Biol* **77**:78–86,  
30 778 Elsevier Ltd (2016).  
31  
32  
33 779 27 Zhao X and Salgado VL, The role of GABA and glutamate receptors in  
34 780 susceptibility and resistance to chloride channel blocker insecticides, *Pestic*  
35 781 *Biochem Physiol* **97**:153–160 (2010).  
36  
37  
38 782 28 Fushiki S, Sugama H, Hamasaki Y and Niwa H, Functional characterization of  
39 783 *Musca* glutamate- and GABA-gated chloride channels expressed independently  
40 784 and coexpressed in *Xenopus oocytes*, *Insect Mol Biol* **15**:773–783 (2006).  
41  
42  
43 785 29 Van Leeuwen T, Vontas J, Tsagkarakou A, Dermauw W and Tirry L, Acaricide  
44 786 resistance mechanisms in the two-spotted spider mite *Tetranychus urticae* and  
45 787 other important Acari: A review, *Insect Biochem Mol Biol* **40**:563–572, Elsevier  
46 788 Ltd (2010).  
47  
48  
49 789 30 Mota-Sanchez D and Wise JC, Arthropod pesticide resistance database, 2020.  
50 790 <http://www.pesticideresistance.org>.  
51  
52  
53 791 31 Xu D, He Y, Zhang Y, Xie W, Wu Q and Wang S, Status of pesticide resistance  
54 792 and associated mutations in the two-spotted spider mite, *Tetranychus urticae*, in  
55 793 China, *Pestic Biochem Physiol* **150**:89–96 (2018).  
56  
57  
58 794 32 Çağatay NS, Menault P, Riga M, Vontas J and Ay R, Identification and  
59  
60

- 1  
2  
3 795 characterization of abamectin resistance in *Tetranychus urticae* Koch  
4 populations from greenhouses in Turkey, *Crop Prot* **112**:112–117, Elsevier  
5 796  
6 797 (2018).  
7  
8 798 33 Ferreira CBS, Andrade FHN, Rodrigues ARS, Siqueira HAA and Gondim MGC,  
9 Resistance in field populations of *Tetranychus urticae* to acaricides and  
10 799  
11 characterization of the inheritance of abamectin resistance, *Crop Prot* **67**:77–83,  
12 800  
13 Elsevier Ltd (2015).  
14 801  
15 802 34 Monteiro VB, Gondim MGC, José JE, Siqueira HAA and Sousa JM, Monitoring  
16 803  
17 *Tetranychus urticae* Koch (Acari: Tetranychidae) resistance to abamectin in  
18 vineyards in the Lower Middle São Francisco Valley, *Crop Prot* **69**:90–96 (2015).  
19 804  
20 805 35 Khajehali J, Van Nieuwenhuysse P, Demaeght P, Tirry L, and Van Leeuwen T,  
21 Acaricide resistance and resistance mechanisms in *Tetranychus urticae*  
22 806  
23 populations from rose greenhouses in the Netherlands, *Pest Manag Sci*  
24 807  
25 **67**:1424–1433 (2011).  
26 808  
27 809 36 Xue W, Snoeck S, Njiru C, Inak E, Dermauw W and Leeuwen V, Geographical  
28 distribution and molecular insights into abamectin and milbemectin cross-  
29 810  
30 resistance in European field populations of *Tetranychus urticae*, *Pest Manag Sci*  
31 811  
32 (2020).  
33 812  
34 813 37 Kwon DH, Yoon KS, Clark JM and Lee SH, A point mutation in a glutamate-gated  
35 chloride channel confers abamectin resistance in the two-spotted spider mite,  
36 814  
37 *Tetranychus urticae* Koch, *Insect Mol Biol* **19**:583–591 (2010).  
38 815  
39 816 38 Mermans C, Dermauw W, Geibel S and Van Leeuwen T, A G326E substitution  
40 in the glutamate-gated chloride channel 3 (GluCl3) of the two-spotted spider mite  
41 817  
42 *Tetranychus urticae* abolishes the agonistic activity of macrocyclic lactones, *Pest*  
43 818  
44 *Manag Sci* **73**:2413–2418 (2017).  
45 819  
46 820 39 Wang X, Puinean AM, O'Reilly AO, Williamson MS, Smelt CLC, Millar NS, *et al.*,  
47 Mutations on M3 helix of *Plutella xylostella* glutamate-gated chloride channel  
48 821  
49 confer unequal resistance to abamectin by two different mechanisms, *Insect*  
50 822  
51 *Biochem Mol Biol* **86**:50–57 (2017).  
52 823  
53 824 40 Yamaguchi M, Sawa Y, Matsuda K, Ozoe F and Ozoe Y, Amino acid residues of  
54 both the extracellular and transmembrane domains influence binding of the  
55 825  
56 antiparasitic agent milbemycin to *Haemonchus contortus* AVR-14B glutamate-  
57 826  
58 gated chloride channels, *Biochem Biophys Res Commun* **419**:562–566, Elsevier  
59 827  
60 828 Inc. (2012).

- 1  
2  
3 829 41 Papapostolou K, Riga M, Charamis J, Skoufa E, Souchlas V, Ilias A, *et al.*,  
4 830 Identification and characterization of striking multiple-insecticide resistance in a  
5 831 *Tetranychus urticae* field population from Greece, *Pest Manag Sci*, Wiley Online  
6 832 Library.  
7  
8  
9 833 42 Nakata Y, Fuse T, Yamato K, Asahi M, Nakahira K, Ozoe F, *et al.*, A single amino  
10 834 acid substitution in the third transmembrane region has opposite impacts on the  
11 835 selectivity of the parasiticides fluralaner and ivermectin for ligand-gated chloride  
12 836 channels, *Mol Pharmacol* **92**:546–555 (2017).  
13  
14 837 43 Furutani S, Okuhara D, Hashimoto A, Ihara M, Kai K, Hayashi H, *et al.*, An L319F  
15 838 mutation in transmembrane region 3 (TM3) selectively reduces sensitivity to  
16 839 okaramine B of the *Bombyx mori* L-glutamate-gated chloride channel, *Biosci*  
17 840 *Biotechnol Biochem* **81**:1861–1867, Taylor & Francis (2017).  
18  
19 841 44 Bryon A, Kurlovs AH, Dermauw W, Greenhalgh R, Riga M, Grbic M, *et al.*,  
20 842 Disruption of a horizontally transferred phytoene desaturase abolishes  
21 843 carotenoid accumulation and diapause in *Tetranychus urticae*, *Proc Natl Acad*  
22 844 *Sci U S A* **114**:E5871–E5880 (2017).  
23  
24 845 45 İnak E, AlpKent YN, Çobanoğlu S, Dermauw W and Van Leeuwen T, Resistance  
25 846 incidence and presence of resistance mutations in populations of *Tetranychus*  
26 847 *urticae* from vegetable crops in Turkey, *Exp Appl Acarol*:343–360 (2019).  
27  
28 848 46 Van Leeuwen T, Van Pottelberge S and Tirry L, Comparative acaricide  
29 849 susceptibility and detoxifying enzyme activities in field-collected resistant and  
30 850 susceptible strains of *Tetranychus urticae*, *Pest Manag Sci* **61**:499–507 (2005).  
31  
32 851 47 Hall TA, BioEdit: a user-friendly biological sequence alignment editor and  
33 852 analysis program for Windows 95/98/NT, 1999.  
34  
35 853 48 Van Laecke K and Degheele D, Carboxylamidases in *Spodoptera exigua*:  
36 854 properties and distribution in the larval body, *Phytoparasitica* **21**:9–21 (1993).  
37  
38 855 49 Fotoukkaiaii SM, Tan Z, Xue W, Wybouw N and Van Leeuwen T, Identification  
39 856 and characterization of new mutations in mitochondrial cytochrome b that confer  
40 857 resistance to bifenazate and acequinocyl in the spider mite *Tetranychus urticae*,  
41 858 *Pest Manag Sci* (2019).  
42  
43 859 50 Robertson JL and Preisler HK, Pesticide Bioassays with arthropods, CRC press  
44 860 (1992).  
45  
46 861 51 Riga M, Bajda S, Themistokleous C, Papadaki S, Palzewicz M, Dermauw W, *et*  
47 862 *al.*, The relative contribution of target-site mutations in complex acaricide

- 1  
2  
3 863 resistant phenotypes as assessed by marker assisted backcrossing in  
4 864 *Tetranychus urticae*, *Sci Rep* **7**:1–12, Springer US (2017).  
5  
6 865 52 Port F, Chen HM, Lee T and Bullock SL, Optimized CRISPR/Cas tools for  
7 866 efficient germline and somatic genome engineering in *Drosophila*, *Proc Natl*  
8 867 *Acad Sci U S A* **111** (2014).  
9  
10 868 53 Gratz SJ, Ukken FP, Rubinstein CD, Thiede G, Donohue LK, Cummings AM, *et*  
11 869 *al.*, Highly specific and efficient CRISPR/Cas9-catalyzed homology-directed  
12 870 repair in *Drosophila*, *Genetics* **196**:961–971 (2014).  
13  
14 871 54 Gratz SJ, Wildonger J, Harrison MM and O'Connor-Giles KM, CRISPR/Cas9-  
15 872 mediated genome engineering and the promise of designer flies on demand, *Fly*  
16 873 (*Austin*) **7** (2013).  
17  
18 874 55 Douris V, Papapostolou KM, Ilias A, Roditakis E, Kounadi S, Riga M, *et al.*,  
19 875 Investigation of the contribution of RyR target-site mutations in diamide  
20 876 resistance by CRISPR/Cas9 genome modification in *Drosophila*, *Insect Biochem*  
21 877 *Mol Biol* **87**:127–135, Elsevier Ltd (2017).  
22  
23 878 56 Abbott W, A method of computing the effectiveness of an insecticide, *J Econ*  
24 879 *Entomol* **18**:256–267 (1925).  
25  
26 880 57 Sterck L, Billiau K, Abeel T, Rouzé P and Van De Peer Y, ORCAE: Online  
27 881 resource for community annotation of eukaryotes, *Nat Methods* **9**:1041, Nature  
28 882 Publishing Group (2012).  
29  
30 883 58 Van Leeuwen T, Van Nieuwenhuysse P, Denholm I, Vanholme B, Tirry L, Nauen  
31 884 R, *et al.*, Mitochondrial heteroplasmy and the evolution of insecticide resistance:  
32 885 Non-Mendelian inheritance in action, *Proc Natl Acad Sci* **105**:5980–5985 (2008).  
33  
34 886 59 Rufener L, Danelli V, Bertrand D and Sager H, The novel isoxazoline  
35 887 ectoparasiticide lotilaner ( Credelio™ ): a non-competitive antagonist specific to  
36 888 invertebrates  $\gamma$  - aminobutyric acid-gated chloride channels ( GABACs ), *Parasit*  
37 889 *Vectors*:1–15, Parasites & Vectors (2017).  
38  
39 890 60 Piraneo TG, Bull J, Morales MA, Lavine LC, Walsh DB, and Zhu F, Molecular  
40 891 mechanisms of *Tetranychus urticae* chemical adaptation in hop fields, *Sci Rep*  
41 892 **5**:1–12 (2015).  
42  
43 893 61 Riga M, Tsakireli D, Ilias A, Morou E, Myridakis A, Stephanou EG, *et al.*,  
44 894 Abamectin is metabolized by CYP392A16, a cytochrome P450 associated with  
45 895 high levels of acaricide resistance in *Tetranychus urticae*, *Insect Biochem Mol*  
46 896 *Biol* **46**:43–53, Elsevier Ltd (2014).

- 1  
2  
3 897 62 Pavlidi N, Tseliou V, Riga M, Nauen R, Van Leeuwen T, Labrou NE, *et al.*,  
4 898 Functional characterization of glutathione S-transferases associated with  
5 899 insecticide resistance in *Tetranychus urticae*, *Pestic Biochem Physiol* **121**:53–  
6 900 60, Elsevier Inc. (2015).  
7  
8  
9  
10 901 63 Wang X, Wang R, Yang Y, Wu S, Reilly AOO and Wu Y, A point mutation in the  
11 902 glutamate-gated chloride channel of *Plutella xylostella* is associated with  
12 903 resistance to abamectin, *Insect Mol Biol* **25**:116–125 (2016).  
13  
14  
15 904 64 Huang X, Chen H and Shaffer PL, Crystal Structures of Human GlyR $\alpha$ 3 Bound  
16 905 to Ivermectin, *Structure* **25**:945-950.e2, Elsevier Ltd. (2017).  
17  
18  
19 906 65 Frenkel L, Muraro NI, Beltrán González AN, Marcora MS, Bernabó G, Hermann-  
20 907 Luibl C, *et al.*, Organization of Circadian Behavior Relies on Glycinergic  
21 908 Transmission, *Cell Rep* **19**:72–85 (2017).  
22  
23  
24 909 66 Xu Z, Liu Y, Wei P, Feng K, Niu J, Shen G, *et al.*, High gamma-aminobutyric acid  
25 910 contents involved in abamectin resistance and predation, an interesting  
26 911 phenomenon in spider mites, *Front Physiol* **8**:1–11 (2017).  
27  
28  
29 912 67 Xu Z, Hu Y, Hu J, Qi C, Zhang M, Xu Q, *et al.*, The interaction between abamectin  
30 913 and RDL in the carmine spider mite: a target site and resistant mechanism study,  
31 914 *Pestic Biochem Physiol* **164**:191–195, Elsevier (2020).  
32  
33  
34 915 68 Taylor-Wells J, Senan A, Bermudez I and Jones AK, Species specific RNA A-  
35 916 to-I editing of mosquito RDL modulates GABA potency and influences agonistic,  
36 917 potentiating and antagonistic actions of ivermectin, *Insect Biochem Mol Biol*  
37 918 **93**:1–11, Elsevier Ltd (2018).  
38  
39  
40  
41 919 69 Lees K, Musgaard M, Suwanmanee S, Buckingham SD, Biggin P and Sattelle  
42 920 D, Actions of agonists, fipronil and ivermectin on the predominant In vivo splice  
43 921 and edit variant ( RDLbd, I/V) of the *Drosophila* GABA receptor expressed in  
44 922 *Xenopus laevis* Oocytes, *PLoS One* **9** (2014).  
45  
46  
47  
48 923 70 Feng XP, Hayashi J, Beech RN and Prichard RK, Study of the nematode putative  
49 924 GABA type-A receptor subunits: Evidence for modulation by ivermectin, *J*  
50 925 *Neurochem* **83**:870–878 (2002).  
51  
52  
53 926 71 Douris V, Denecke S, Van Leeuwen T, Bass C, Nauen R, and Vontas J, Using  
54 927 CRISPR/Cas9 genome modification to understand the genetic basis of  
55 928 insecticide resistance: *Drosophila* and beyond, *Pestic Biochem Physiol*  
56 929 **167**:104595, Elsevier (2020).  
57  
58  
59  
60 930 72 Bajda S, Dermauw W, Panteleri R, Sugimoto N, Douris V, Tirry L, *et al.*, A

- 1  
2  
3 931 mutation in the PSST homologue of complex I (NADH:ubiquinone  
4 oxidoreductase) from *Tetranychus urticae* is associated with resistance to METI  
5 932 acaricides, *Insect Biochem Mol Biol* **80**:79–90, Elsevier Ltd (2017).  
6 933  
7  
8 934 73 Dermauw W, Jonckheere W, Riga M, Livadaras I, Vontas J and Van Leeuwen  
9 T, Targeted mutagenesis using CRISPR-Cas9 in the chelicerate herbivore  
10 935 *Tetranychus urticae*, *Insect Biochem Mol Biol* **120**:103347, Elsevier (2020).  
11 936  
12  
13 937 74 Bajda S, Riga M, Wybouw N, Papadaki S, Ouranou E, Fotoukkaia SM, *et al.*,  
14 938 Fitness costs of key point mutations that underlie acaricide target-site resistance  
15 939 in the two-spotted spider mite *Tetranychus urticae*, *Evol Appl* **11**:1540–1553  
16 940 (2018).  
17  
18  
19  
20 941 75 Samantsidis GR, Panteleri R, Denecke S, Kounadi S, Christou I, Nauen R, *et al.*,  
21 942 “What I cannot create, I do not understand”: functionally validated synergism of  
22 943 metabolic and target site insecticide resistance, *Proceedings Biol Sci*  
23 944 **287**:20200838 (2020).  
24  
25  
26  
27  
28  
29  
30  
31  
32  
33  
34  
35  
36  
37  
38  
39  
40  
41  
42  
43  
44  
45  
46  
47  
48  
49  
50  
51  
52  
53  
54  
55  
56  
57  
58  
59  
60

946 **9 TABLES**947 **Table 1. Toxicity of abamectin to adult females of backcrossed lines and their parental strains**

	Strain	Genotype	Slope(±SE)	LC <sub>50</sub> (95% CI) (mg a.i./L)	RRs <sup>a,b</sup> (95%CI)
<b>♀SR6 x♂TR2 (BC1)</b>					
Backcrossed lines	TRA_R1	321T	2.85 (±0.28)	6.00 (5.36-6.80)	44.14 (37.38-52.12)*
	TRA_R2	321T	3.17 (±0.31)	8.10 (7.08-9.04)	59.51 (50.31-70.39)*
	TRA_R3	321T	3.67 (±0.31)	5.85 (5.32-6.38)	42.70 (37.08-49.78)*
	TRA_C1	I321	2.51 (±0.22)	0.15 (0.14-0.18)	1.13 (0.95-1.34)
	TRA_C2	I321	2.71 (±0.22)	0.13 (0.12-0.15)	0.98 (0.83-1.16)
Parental strains	SR6_BC1	I321	2.84 (±0.23)	0.14 (0.12-0.15)	1.00
	TR2	321T	2.52 (±0.25)	11.19 (8.57-14.50)	82.26 (69.24-97.72)*
<b>♀SR6 x♂IT6 (BC2)</b>					
Backcrossed lines	ITA_R1	321T	4.08 (±0.30)	0.42 (0.38-0.47)	1.80 (1.57-2.06)*
	ITA_R2	321T	4.63 (±0.44)	0.33 (0.30-0.36)	1.39 (1.21-1.59)*
	ITA_R3	321T	4.71 (±0.42)	0.34 (0.30-0.37)	1.42 (1.24-1.64)*
	ITA_C1	I321	3.36 (±0.30)	0.22 (0.19-0.26)	0.94 (0.81-1.10)
	ITA_C2	I321	4.82 (±0.41)	0.18 (0.15-0.21)	0.75 (0.66-0.87)*
Parental strains	ITA_C3	I321	4.03 (±0.31)	0.26 (0.23-0.31)	1.11 (0.96-1.28)
	SR6_BC2	I321	3.31 (±0.25)	0.24 (0.21-0.26)	1.00
	IT6	321T	3.33 (±0.22)	24.96 (22.76-27.20)	105.5 (92.02-120.9)*

948 <sup>a</sup>The resistance ratio (RR) compared to the susceptible strain SR6949 <sup>b</sup>An asterisk (\*) indicates the RR was considered significantly different from 1 based on non-overlap of 95% CI (PoloPlus LeOra Software).<sup>50</sup>

950

951

952

953 **Table 2. Log-dose probit-mortality data for abamectin tested against larvae of *Drosophila* genome modified strain I321T vs**  
 954 **wild-type control (nos.Cas9).** LC<sub>50</sub> values are given in mg a.i./L. The resistance ratio (RR) is calculated by dividing the LC<sub>50</sub> of strain  
 955 I321T by the LC<sub>50</sub> of the wild type strain nos.Cas9.

Compound	Strain	Slope ± SE	LC <sub>50</sub> (95% CI) (mg a.i./L)	RRs <sup>a,b</sup> (95% CI)
abamectin	nos.Cas9	7.32 (±1.34)	0.018 (0.014-0.020)	1
	I321T	3.70 (±0.40)	0.048 (0.039-0.055)	2.66 (2.30-3.06)*

956 <sup>a</sup>The resistance ratio (RR) compared to the wild type strain nos.Cas9.

957 <sup>b</sup>An asterisk (\*) indicates the RR was considered significantly different from 1 based on non-overlap of 95% CI (PoloPlus LeOra Software).<sup>50</sup>

958

959 **Table 3. L-glutamic acid and abamectin responses of wild- and mutant GluCl3 expressed in *Xenopus* oocytes.** Data represent  
 960 the mean of 8 oocytes ± SEM.

	Wild-type			GluCl3 I321T		
	EC <sub>50</sub> (μM)	pEC <sub>50</sub>	n <sub>H</sub> <sup>†</sup>	EC <sub>50</sub> (μM)	pEC <sub>50</sub>	n <sub>H</sub> <sup>†</sup>
L-glutamic acid	476.4	3.32 ± 0.01	2.34 ± 0.14	311.3	3.51 ± 0.02	2.42 ± 0.31
abamectin	0.447	6.32 ± 0.12	0.97 ± 0.23	-	-	-

961 <sup>†</sup>n<sub>H</sub>: Hill coefficient

962

963

964

965

966

967



968 **Table 4. GABA and abamectin responses of three wild-type *T. urticae* RdlS expressed in *Xenopus* oocytes.** Data are the mean  
 969 of 6-8 oocytes  $\pm$  SEM

	GABA				Abamectin			
	n <sup>†</sup>	EC <sub>50</sub> ( $\mu$ M)	pEC <sub>50</sub>	n <sub>H</sub> <sup>‡</sup>	n <sup>†</sup>	IC <sub>50</sub> ( $\mu$ M)	pIC <sub>50</sub>	n <sub>H</sub> <sup>‡</sup>
Rdl1	8	15.5	4.81 $\pm$ 0.007	5.61 $\pm$ 0.56	8	0.102 <sup>a</sup>	6.98 $\pm$ 0.34	-0.47 $\pm$ 0.24
					6	0.058 <sup>b</sup>	7.23 $\pm$ 0.17	-0.45 $\pm$ 0.11
					6	0.179 <sup>c</sup>	6.74 $\pm$ 1.98	-0.21 $\pm$ 0.51
Rdl2	6	68.6	4.16 $\pm$ 0.034	1.56 $\pm$ 0.16	6	0.226	6.64 $\pm$ 0.21	-1.07 $\pm$ 0.43
Rdl3	6	139.8	3.85 $\pm$ 0.035	3.36 $\pm$ 0.65	6	0.502	6.29 $\pm$ 0.35	-0.49 $\pm$ 0.18

970 <sup>†</sup>number of oocytes

971 <sup>‡</sup>n<sub>H</sub>: Hill coefficient

972 <sup>a</sup>Co-application of GABA (EC<sub>50</sub>) and abamectin

973 <sup>b</sup>Co-application of GABA (EC<sub>5</sub>) and abamectin

974 <sup>c</sup>Co-application of GABA (EC<sub>90</sub>) and abamectin

## 975 10 FIGURES LEGENDS

976 **Figure 1. Identification of an I321T mutation in GluCl3 of abamectin resistant *T.***  
 977 ***urticae* strains.** a) Individual GluCl channel subunit, consisting of four transmembrane  
 978 (TM) domains; the I321T mutation (indicated with a red star) found in abamectin  
 979 resistant *T. urticae* is located in TM3; b) Alignment of TM3 of *T. urticae GluCl1* and  
 980 *GluCl3* with GluCl of *Drosophila melanogaster*, *Plutella xylostella* and *Caenorhabditis*  
 981 *elegans*. The I321T mutation is indicated with a red star, while the A309V mutation in  
 982 *P. xylostella GluCl* and G314D / G326E in *T. urticae GluCl1 / GluCl3*, which were  
 983 previously associated with abamectin resistance,<sup>14,37,38,63</sup> are indicated with a square  
 984 and triangle, respectively. *C. elegans GluCl $\alpha$*  residues that were previously shown to  
 985 be involved in ivermectin binding are underlined.<sup>7</sup> An 80% threshold was used for  
 986 identity (black background) and similarity shading (grey background). Abbreviation of  
 987 species names: Tu, *T. urticae*; Ce, *C. elegans*; Dm, *D. melanogaster*; Px, *P. xylostella*;  
 988 c) GluCl channels consist of five GluCl subunits, which in *T. urticae* might be encoded  
 989 by the same gene (e.g. *GluCl3* carrying the I321T mutation) or can be encoded by  
 990 different genes (e.g. *GluCl3* I321T and *GluCl1*) or, as was shown for *D.*  
 991 *melanogaster*,<sup>12</sup> ivermectin receptors might be formed that consist of both GluCl and  
 992 Rdl subunits.

993  
 994 **Figure 2. L-glutamic acid and abamectin activation of GluCl3 WT and GluCl3**  
 995 **I321T expressed in *Xenopus* oocytes.** a): Examples of electrical current responses.  
 996 The period of L-glutamic acid application time is indicated by the bar above the trace  
 997 as well as the concentrations applied (mM); b): Examples of electrical current  
 998 responses for abamectin. The period of application is indicated by the bar above the  
 999 trace as well as the concentrations applied; c): Abamectin potentiation of L-glutamic  
 1000 induced currents; perfusion of GluCl3 WT, GluCl3 I321T and GluCl3 G326E injected  
 1001 oocytes with 1 mM of L-glutamic acid followed by co-application of 1 mM L-glutamic  
 1002 acid and 100 nM abamectin; d) L-Glutamic acid dose-response curves for the  
 1003 activation of wild-type and I321T GluCl3; e): Abamectin dose-response curves for the  
 1004 activation of wild-type and I321T GluCl3; Error bars indicate SEM (n=8).

1005  
 1006 **Figure 3. Antagonistic activity of abamectin on the Rdl1, Rdl2 and Rdl3 GABA**  
 1007 **receptors expressed in *Xenopus* oocytes.** a): A current trace when abamectin was

1  
2  
3 1008 administered to Rdl1; b): Current traces from a cumulative exposure to increasing  
4 1009 dosage of abamectin obtained for a *Xenopus oocyte* expressing Rdl1. The bars  
5 1010 indicate the time period of co-application of GABA (15  $\mu$ M) and increasing  
6 1011 concentrations of abamectin (1 nM - 10  $\mu$ M); c): GABA dose-response curves for the  
7 1012 activation of Rdl1, Rdl2 or Rdl3; d): Inhibition dose-response curve measured for  
8 1013 abamectin obtained from oocytes expressing Rdl1, Rdl2 or Rdl3. Error bars indicate  
9 1014 SEM (n=6-8).  
10  
11  
12  
13  
14  
15  
16  
17  
18  
19  
20  
21  
22  
23  
24  
25  
26  
27  
28  
29  
30  
31  
32  
33  
34  
35  
36  
37  
38  
39  
40  
41  
42  
43  
44  
45  
46  
47  
48  
49  
50  
51  
52  
53  
54  
55  
56  
57  
58  
59  
60

For Peer Review

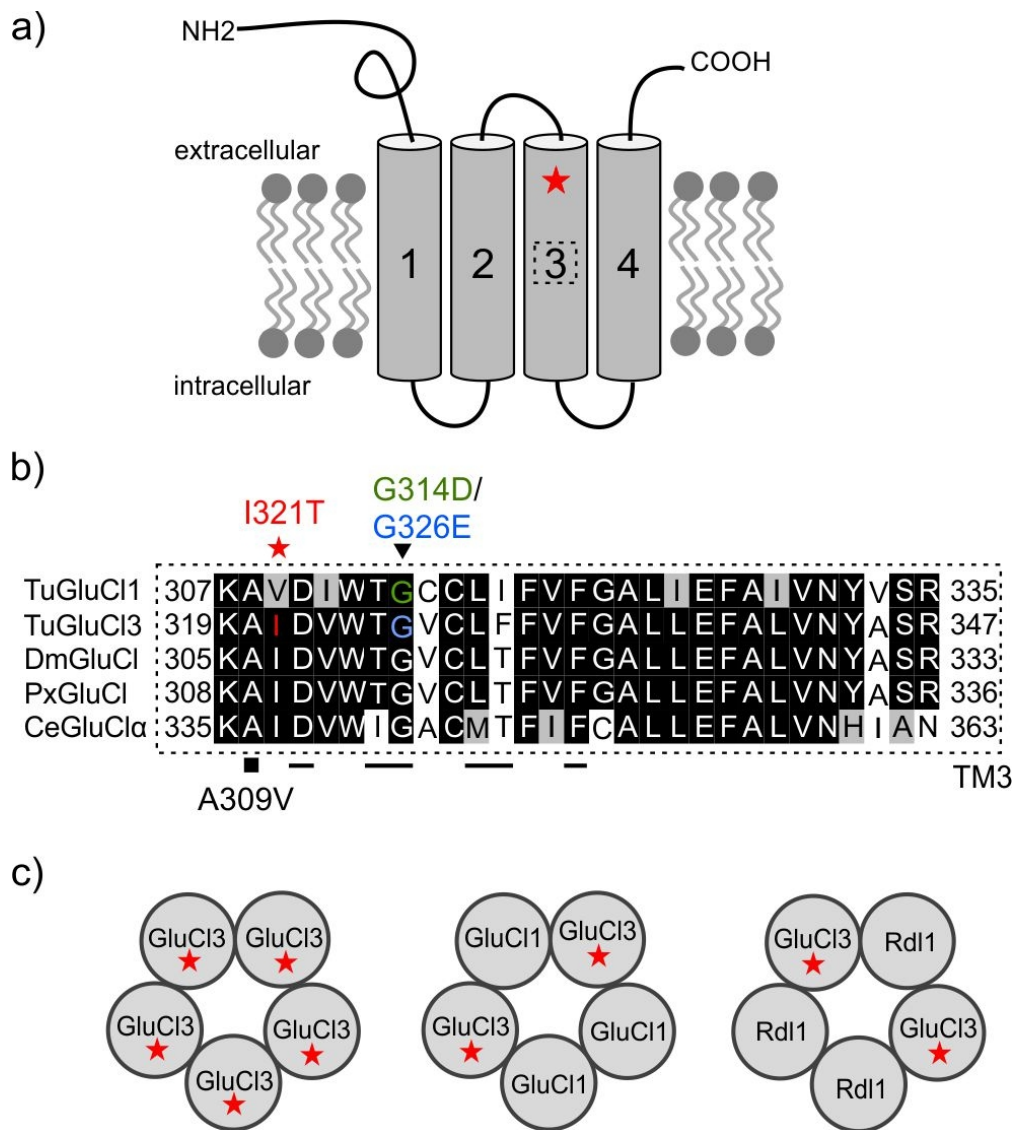


**Figure 1. Identification of an I321T mutation in GluCl3 of abamectin resistant *T. urticae* strains.**

a) Individual GluCl channel subunit, consisting of four transmembrane (TM) domains; the I321T mutation (indicated with a red star) found in abamectin resistant *T. urticae* is located in TM3; b) Alignment of TM3 of *T. urticae* GluCl1 and GluCl3 with GluCl of *Drosophila melanogaster*, *Plutella xylostella* and *Caenorhabditis elegans*. The I321T mutation is indicated with a red star, while the A309V mutation in *P. xylostella* GluCl and G314D / G326E in *T. urticae* GluCl1 / GluCl3, which were previously associated with abamectin resistance,<sup>14,37,38,61</sup> are indicated with a square and triangle, respectively. *C. elegans* GluClα residues that were previously shown to be involved in ivermectin binding are underlined.<sup>7</sup> An 80% threshold was used for identity (black background) and similarity shading (grey background). Abbreviation of species names: Tu, *T. urticae*; Ce, *C. elegans*; Dm, *D. melanogaster*; Px, *P. xylostella*; c) GluCl channels consist of five GluCl subunits, which in *T. urticae* might be encoded by the same gene (e.g. GluCl3 carrying the I321T mutation) or can be encoded by different genes (e.g. GluCl3 I321T and GluCl1) or, as was shown for *D. melanogaster*,<sup>12</sup> ivermectin receptors might be formed that consist of both GluCl and Rdl subunits.

83x93mm (300 x 300 DPI)

1  
2  
3  
4  
5  
6  
7  
8  
9  
10  
11  
12  
13  
14  
15  
16  
17  
18  
19  
20  
21  
22  
23  
24  
25  
26  
27  
28  
29  
30  
31  
32  
33  
34  
35  
36  
37  
38  
39  
40  
41  
42  
43  
44  
45  
46  
47  
48  
49  
50  
51  
52  
53  
54  
55  
56  
57  
58  
59  
60

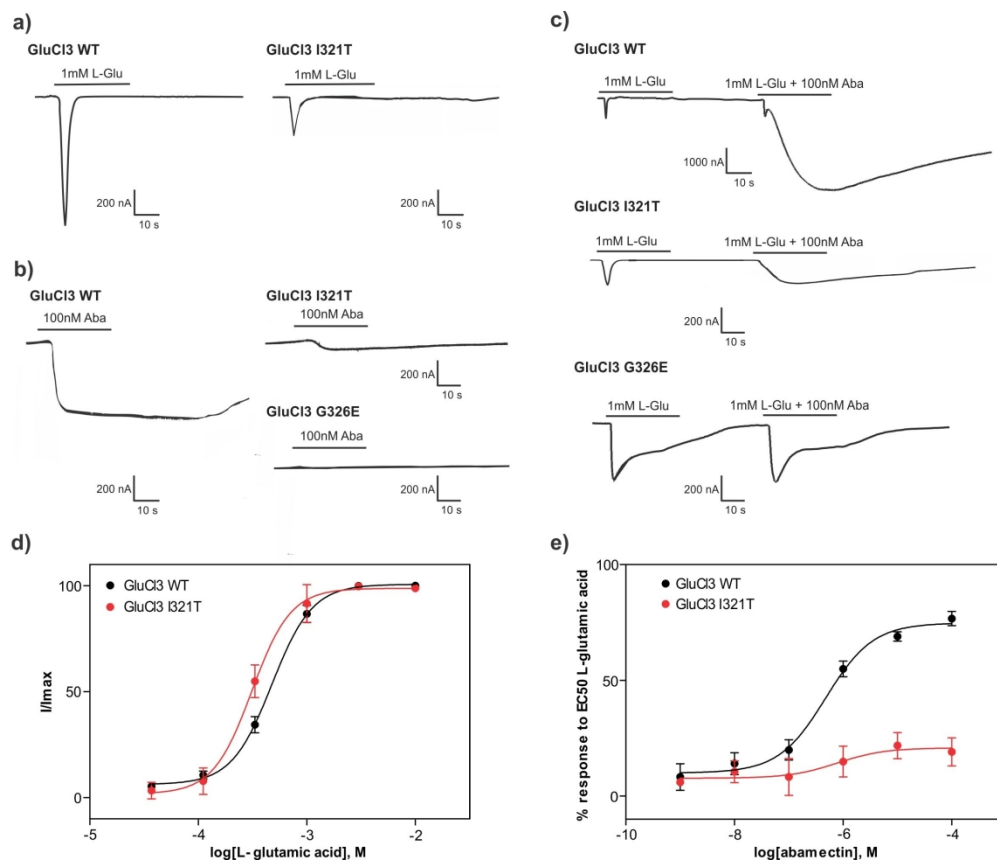


**Figure 2. L-glutamic acid and abamectin activation of GluCl3 WT and GluCl3 I321T expressed in *Xenopus oocytes*.** a): Examples of electrical current responses. The period of L-glutamic acid application time is indicated by the bar above the trace as well as the concentrations applied (mM); b): Examples of electrical current responses for abamectin. The period of application is indicated by the bar above the trace as well as the concentrations applied; c): Abamectin potentiation of L-glutamic induced currents; perfusion of GluCl3 WT, GluCl3 I321T and GluCl3 G326E injected oocytes with 1 mM of L-glutamic acid followed by co-application of 1 mM L-glutamic acid and 100 nM abamectin; d) L-Glutamic acid dose-response curves for the activation of wild-type and I321T GluCl3; e): Abamectin dose-response curves for the activation of wild-type and I321T GluCl3; Error bars indicate SEM (n=8).

199x169mm (300 x 300 DPI)

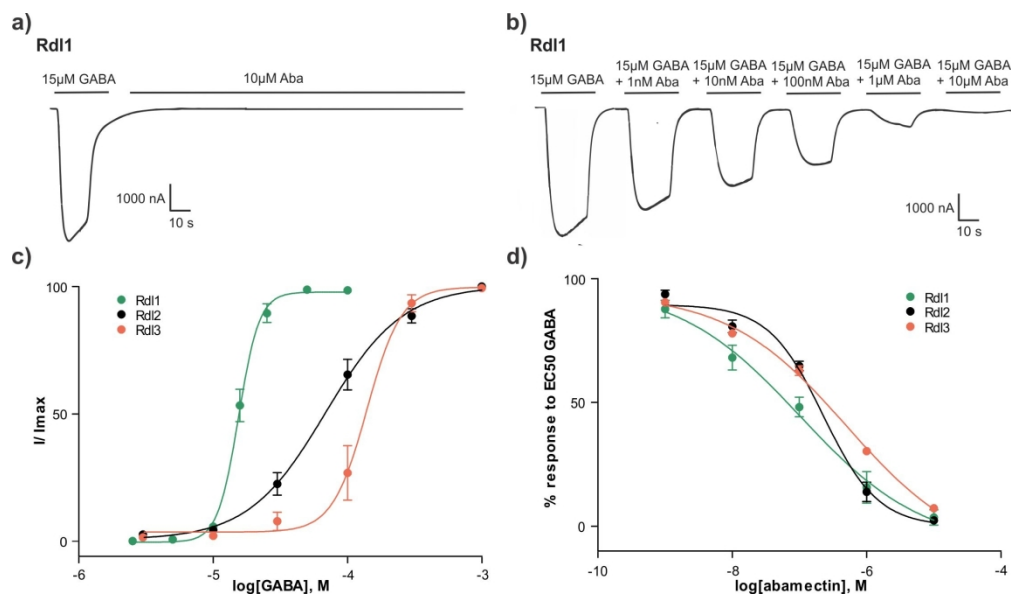


**Figure 3. Antagonistic activity of abamectin on the Rdl1, Rdl2 and Rdl3 GABA receptors expressed in *Xenopus oocytes*.** a): A current trace when abamectin was administered to Rdl1; b): Current traces from a cumulative exposure to increasing dosage of abamectin obtained for a *Xenopus oocyte* expressing Rdl1. The bars indicate the time period of co-application of GABA (15 μM) and increasing concentrations of abamectin (1 nM - 10 μM); c): GABA dose-response curves for the activation of Rdl1, Rdl2 or Rdl3; d): Inhibition dose-response curve measured for abamectin obtained from oocytes expressing Rdl1, Rdl2 or Rdl3. Error bars indicate SEM (n=6-8).

188x109mm (300 x 300 DPI)

**File S1 - Sequences of *T. urticae* GluCl and Rdl constructs that were ligated into a pUC57 vector (FASTA format).**

>TuGluCl3

ATTGTAATACGACTCACTATAGGGCGAATTAATTCGAGCTCGGTACCCAGCTTGCTTGTTCTTTTTGC  
 AGAAGCTCAGAATAAACGCTCAACTTTGGCAGATCAATTCGCCGGGATCCGAATTCTCTAGAGCAA  
 GCTTGCCACCATGCTGTGTCTGCCTGGACCAAAGTACCACATTACTTTTTATCTGCTGATCTACTTCAG  
 CGATTTTATTATCATCCCTTGGCTGCTGAATCTGCCATTTACTAGCGGAAGTGCCTCTTTTAGGGAAACA  
 GGAGAAGAAAATTCTGGATTCCATCATTGGACAGGGAGCTTACGATAGAAGGATCAGACCTTCTGG  
 ACTGAATGCTTCCGCTGAAGGAGATGGACCATGCATTGTGTCCATCAACATTTATCTGAGGTCCATTA  
 GTAAGATTAGCGATCTGGATATGGAATATTCCGTGCAGATTACATTCAGAGAGGAATGGAAGGATTC  
 CAGGCTGGTGTACAGAGATCCAAGCGAGAAAATTAGATACCTGACACTGACTGATCCTGATAGGATC  
 TGGAAGCCTGATGTGTTTTTCAAAACGAGAAAGAAGGACATTTCCACAACATCATATGCCAAATG  
 TGCTGCTGAGAATTGGAAGCGATGGAGGAGTGTGTACAGCATCAGACTGAGCCTGATTCTGTCTCTG  
 TCCTATGAACCTGAAATACTATCCACTGGATAAGCAGAATTGCTACATCAAGATGGCCAGCTACGGA  
 TATACAACTGAAGATCTGGTGTTTCATGTGGAAGAAAATGATCCAGTGCAGGTGACAAAACAGCTGC  
 ATCTGCCTACATTCGCACTGGCTGATTATCACTGAGTATTGCACATCCAGAACTAACACAGGAGAG  
 TATTCCTGCGTGCAGGTGAAACTGATCTTTAGAAGGGAGTTCAGCTATTACCTGATCCAGATTTACAT  
 CCCATGCATTATGCTGGTGATTGTGAGCTGGGTGAGTTTTTGGCTGGACCCAAACGAATTCCTGCA  
 AGAGTGTCCCTGGGAGTGACAACACTGCTGACTATGGCAACACAGATCAGTGAATTAACGCCAGC  
 CTGCCACCTGTGTCTTATATTAAGGCAATCGATGTGTGGACAGGAGTGTGCCTGTTTTTCGTGTTTGG  
 AGCCCTGCTGGAGTTTGCCTGGTGAACACTACGCCAGTAGATCTGATGCACATAGGGCTGCAAGAAA  
 AAGGAGAGCAGAGAATCAGCAGCAGCAGGTGCAGCAGGTGCTGGGAGGGGGGAGGAAGCGCATT  
 GGATTCCTGAGGGGGGAGGGGGGAGGGGGGAGGGGGGACTGGGAAACATGGGAAACCCA  
 GGATACGGAATGACTGGAGGGGGAATGGGATTTCCACCTCCACCACCAAAATGGGATTCCAATCCTT  
 GGGAACCTCACCAGCCTATGCCTCCACACCCAATGGACCCTCCACCTGCAACAAAGTGGGAGGCAAG  
 AGTGGATCTGAAACCTAGAGGATTCCAGTATTCCAGCGATAATTTTCACTCTCCAGAGCTAGTTACG  
 TGATGAAACCAGTGTGCTGAGAGGACCACAGCCTAATCCACCACCTGCAACAATAAATTCATCAGGT  
 GGAAGTGAGAACTGCACCATAACAACAGAATTGCCTGACAAGGTGGTTTGCCGCATTCCAGACAAG  
 GAGCAAAAGAATCGATGTGCTGGCTAGAATCCTGTTCCACTGATGTTCAAGCCTGTTCAACGTGGTG  
 TATTGGATTACATACGTGGTGATTCTGGGATAAAGCTTACCAGCCTCAAGAACCCCGAATGGAGT  
 CTCTAAGCTACATAATACCAACTTACACTTTACAAAATGTTGTCCCCCAAATGTAGCCATTCTGATCT  
 GCTCCTAATAAAAAGAAAGTTTCTTACATTCTAAAAAAAAAAAAAAAAAAAAAAAAACCCCCCCTGC  
 AGGCGGCCGCTCGAGGCTAGCTTGAGTATTCTATAGTGTACCTAAATAGCT

>TuRdl1

ATTGTAATACGACTCACTATAGGGCGAATTAATTCGAGCTCGGTACCCAGCTTGCTTGTTCTTTTTGC  
 AGAAGCTCAGAATAAACGCTCAACTTTGGCAGATCAATTCGCCGGGATCCGAATTCTCTAGAGCAA  
 GCTTGCCACCATGATGATGCTGATGCTGCTGCTGAAGCCTATCAGCCTGCTGTGTTCCCTGT  
 GTTGCCTGCCACTGCTGTCCCTGACTATGCTGATCATCCCTGCTTTTGGACACAACCTGGCAGTCTCAT  
 GGATACCAGGGAGATCAGCCTCACGAGTTTGGACACACTAATGGAGATATCGGAAGTAATATCTCTC  
 AGATCCTGAACAGCTTTTTCTTCCGGATATGATAAAAGAGTGAGACCTAATGAGGACCTCCA  
 GTGAAAGTGGGAGTGACAATGCACATTCTGACAATTTCTAGTGTGAGCGAAGTGCAGATGGATTTCA  
 CAGCAGATTTCTATTTTAGACAGCTGTGGAGGGATAGCAGGCTGAGCTTAAAGGCTAGACACGGAAT  
 TTCCAGATTCTGGTGGATGCCGAGGTGGCCGATAAGATTTGGGTGCCTGATACTTTCTTCGTAATG  
 AAAAGCAGGCATATTTCCATGAAGCTACTACTAAGAATACATTTCTGAGGATTTCTCACGATGGACA



1  
 2  
 3 GGTGCTGAGAAGCATCAGACTGACAGTGACTGCTTCTGTCCAATGAACCTGCAATATTTCCCAATG  
 4 GATAGGCAGAAGTGTAATATCGAAATCGAAAGTTATGGATACTCCATGACTGATATCATTTACAAC  
 5 GGGTGGATGAAAACGCAGTGAAAATCGATTCTAATCTGATGCTGCCTCAGTTTAGCATCGCTCCATT  
 6 AGACAGTCTTGAAATATATTAGTCTGACTACTGGAACTACAGTAGGCTGATGTGCGAAATCCAGC  
 7 TGACAAGAAGCATGGGATATTACATGATCCAGATCTACGTGCCAGCTAGTCTGATCGTGATTATCTCT  
 8 TGGGTGAGTTTTTGGCTGCACAGAAACGCAACACCTGCAAGAGTGCACCTGGGAGTGATCACTGTG  
 9 CTGACAATGACTACACTGATGTCTAGCACAAACAGCCAGCTGCCAAAGATCTCCTACGTGAAGTCTAT  
 10 TGATGTGTTTCTGGGAACTTGTTTTGTGATGGTGTTCGCTGCACTGCTGGAATATGCAGCCGTGGGA  
 11 TACATCGGAAAGAGGATTTCTATGAGGAAGAAGAGTTTCAGCAGCTGGCTAAAGCAGCCGAAGAG  
 12 AAAAGAAGAAAACCTGGTGGAAAGCTGCCGCCGCTGCCGCAGCAGCTGCTGCTGCTGCAACTCCTGT  
 13 GAACCAATCCACCTGTCTTCTCTGATCCTAGCGGACCACAGAGTCACCCAATTAAGTCAACAATAG  
 14 TAACAACCCATCCAGTATTAACATCAGTACTACAACAACCCAATGAATATCAACAACATCAATAGTA  
 15 ATGGAATAACAACAATAACAACAACAACCCAATAATAACAATCTGAATAACATCAACAA  
 16 CTCCAATAACGGATCTTCTATCACTACACTGACAACCTGTGGCAACAGCTGCCGGAGGAAATGTGAGT  
 17 TCTGTGGGACCAATGGGAAGCACAGGAAGTACTTTAACCAGACTACAGGACAGCTGGTGGTGGAT  
 18 AGTGCTCTGCATGGATCTGGACTGACAGGAACATCCGTGTGCAGCGCTAGTGCCACAGTGGGAGTG  
 19 CCTAGCGTGCCTAAACATCAGCTGTATCAGCAGCAGCAGGGACAGCCACATCACCACCTGACACATC  
 20 ATCAGATCTAGTTATCAGCAGCATCATCAGCATCTGCAACAGCAGCTGCAACAGCAGCAGCAGCA  
 21 GCACCAGAGCATCGGAACACTGACTAGCGTGAGCAACCTGGGAGTGGGACTGTCTGTGCCTAGCAA  
 22 CCTGGTGACATACGATTTCTCTGGAAATGGACTGAGCGGAGGATCTGGAAATCTGATGATGACTACA  
 23 AACCTGAAATGATTAATTGTAGCCTGGGACCTGGAGGACATGGAGGATCTATGGGATCTATGCCAC  
 24 TGGGATGTAGCAGAGATGATCAGGATCAGGAAACTCTGGTGAAGTCAAGTGGGACATTATGCTACTCT  
 25 GAGAAGGCCTCTGCTGGATAGATCTCCCTGCCTGTAAGGGAGCTGCTAGTAGTGGAGTGGTGGG  
 26 AGTGACTGGAGGAACTAGTGTGGGAAGTACTGGAGGAAGTATGCCTGGACAGCCTAACAGAAAGC  
 27 AGTTTCTGCCTCATAGACCTCAGGAAGTGGGCTGGAAATGGTGGGATCTAAAATGACTCCTGTGGC  
 28 TCAGACTTCTGGAAGTATGGATGGAGTGAACCATCATCAGCCTGGAGGACTGAGCAGTTCAGTATT  
 29 GGAAGAATCCCAGGACACTTCACAATAATCTGCACAGGTTACTGCCGTGCCACCTAAGAACCTGA  
 30 ATAATCTGTTTGGAGTGTCCCTTCTGATATCGATAAGTATAGTAGGGTGGTGTTCCTGTGTGCTTC  
 31 GTGTGCTTTAACCTGATGTACTGGATTATTTTCTGCACATCAGCAGCATCCTGGAACCAGGAGCAGA  
 32 TGAAGAGTCTGAAAGCTTACCAGCCTCAAGAACACCCGAATGGAGTCTTAAGCTACATAATACCA  
 33 ACTTACACTTTACAAAATGTTGTCCCCAAAATGTAGCCATTTCGATCTGCTCCTAATAAAAAGAAAG  
 34 TTTCTTACATTCTAAAAAAAAAAAAAAAAAAAAAAAAACCCCCCCTGCAGGCGGCCGCTCGAGGCTA  
 35 GCTTGAGTATTCTATAGTGTACCTAAATAGCT

>Tu\_Rdl2

46 ATTGTAATACGACTCACTATAGGGCGAATTAATTCGAGCTCGGTACCCAGCTTGCTTGTTCTTTTGC  
 47 AGAAGCTCAGAATAAACGCTCAACTTTGGCAGATCAATTCGCCGGGATCCGAATTCTCTAGAGCAA  
 48 GCTTGCACCATGATGATTAATAGGCTGAATCAGTGGATCTTTGTGCTGATTATCATTATGTTAATA  
 49 AATTTAACCTGATCTTTACTCTGAATGAGGAAGAAGATGTGATTGAAAAGGGAAATGCACTGGGACA  
 50 GAACATCACAAAGATTCTGAACGCATTTTTAGTTCCGGATACGATAAAAAGAGTGAGACCAAATAT  
 51 GGAGGACCACCTGTGGAAGTGGGAATCTCCGTGTACTTTACTTCTATCAGCTCTGTGAGCGAAGTGA  
 52 AAATGGATTTACAAGCGATTTCTACTTCAGGCAGGAGTGGAAAGATCCTAGACTGAGCTTCGATCC  
 53 TCTGCCAGGAATCAGCAATCTGTATGTGGGAGCTGAAGTGGCTAAAAAGATCTGGGTGCCTGATACT  
 54 TTCTTTGCAAACGAGAAGCAGGCATATTTCCACGTGGCAACTACACCTAATAGGTTTCTGAGGATTGC  
 55 CTTTAGCGGACTGATTTACCAGTCTATTAGGCTGACAGTGAAGTGGCTTCTGCCCCAATGAGCCTGCAAT  
 56 ATTTTCTATGGATAGGCAGGCTTGTTCATCGAGATTGAAAGCTATGGATACTCCATGAGGGATATC  
 57 AAATATGTGTGGCTGAACGGAAACAAGTCCGTGGATGTGCAGGGAGATGTGACTGCCTCAGTTC

1  
 2  
 3 AAGATCATGGGACATGAGCAGGAATCCGCTATTGCTGCACTGACAACCTGGAACTACTCCAGACTGA  
 4 TCTGTAAGATTAAGTTTAGCAGGTCCCTGGGATTTTATCTGATCCAGATTTATATCCCTGCCTCTCTGA  
 5 TTGTGGTGATCTTTGGGTGTCCTTTGGCTGCATAGAAACGCAACACCTGCAAGAGTGAGCCTGGG  
 6 AGTGACAACAGTGCTGACAATGACTACACTGATGTCCTCTACAAACGCACAGCTGCCAAAAATCTCCT  
 7 ACATTAAGCATTGATGTGTTCTGGGAACATGTTTCGTGATGGTGTTTCGCATCCCTGCTGGAATAC  
 8 GCAACAGTGGGATATCTGGGAAAGAGAATTGCCATGAGAAAAAGCAGAATCGAGCAGCTGACTAA  
 9 GCTGGCAGATGAGCATAGGAAAAAGTGCGCAGCTGCTGCCGCAGCCGCAGATGCAGCTGTGGCTG  
 10 AACAGTCCGCTGCACAGGTGCCTCCACAGCTGATTTGCGCAACAACAGGACTGCCACTGGACCCAGC  
 11 ACTGCAACTGCCATGTGGAATCAAAAACCCTGTGCATCACCAGGGAAACAGGTGTATCGGAGGACC  
 12 TCCACCAAAAATGGTGTATGGAGGATGCCACAGAAGATGAACTCCAGGATTCTGGAAGCAAAACA  
 13 GTCCGAAAAATGATGAACGAAGCATCCAGTATGACTCTGGGAGGGGGAGGGGGACCTGGAAATC  
 14 AGCCTCCACCTACTCCAGTGCCATTTGGACCTAAAGATCCAAACAGAATGCTGGGAGTGAGCCCTTC  
 15 CGATATCGATAAGTACAGTAGGGTGGTGTTCCTGTGTGTTTCATCTGTTTTAACCTGATGTACTGGA  
 16 TCGTGTATATGCACATTAGCGCATCCAGTAGCCCAAACCTAAAGCTTACCAGCCTCAAGAACACCCG  
 17 AATGGAGTCTCTAAGCTACATAATACCAACTTACACTTTACAAAATGTTGTCCCCAAAATGTAGCCA  
 18 TTCGTATCTGCTCCTAATAAAAAGAAAGTTTCTTACATTCTAAAAAAAAAAAAAAAAAAAAACCCC  
 19 CCCCCTGCAGGCGGCCGCTCGAGGCTAGCTTGAGTATTCTATAGTGTACCTAAATAGCT

24  
 25 >TuRdI3

26 ATTGTAATACGACTCACTATAGGGCGAATTAATTCGAGCTCGGTACCCAGCTTGCTTGTTCTTTTGC  
 27 AGAAGCTCAGAATAAACGCTCAACTTTGGCAGATCAATTCCCCGGGGATCCGAATTCTCTAGAGCAA  
 28 GCTTGCCACCATGATGATTAACAGGCTGAATCAGTGGATCTTCGTGCTGATTATCGTGATGTTCAACA  
 29 AGTTTAACCACATTTTTACTGTCTGATTTTGTGTTGGGAGATAAGGGAAACGCACTGGGACAGAA  
 30 CATCACAAGGATTCTGAACGCCTTTTCGCCGAGGATATGATAAAAGGGTGAGACCAAACACTACGGA  
 31 GGACCTCCAGTGGAGATTGGAGTGAGCATGCATATTATCTCCATTAGCACTGTGTCTGAAGTGCAGA  
 32 TGGATTTCACTCCGATTTCTACTTTAGGCAGTTTTGGGAAGATCCTAGGCTGGCCTTTATTCCTCTGC  
 33 CTAGAATTACTGAGCTGTACGTGGGAGCTGAAGTGGCTGATAGGATCTGGGTGCCAGATACTTTCTT  
 34 TGCCAACGAGAAGTCCGCATCTTTCCATTTTCGCTACTACAAAAACACTTTTCTGAGGATCGGAAGTA  
 35 ATGGAGAAGTGTGTTAGAAAGCATTAGGCTGACAGTGACAGCTTCTGCCAATGGAGCTGCAATACTT  
 36 TCCTATGGATAGACAGAAGTGCTCTCTGGAGATCGAGAGCTACGGATACAGCATGAGCGATATGAT  
 37 CTATATTTGGAGGGAAGGAAAGAAAAGCATCAGGATGAACTCCGATCTGTCTCTGCCACAGTTTAAA  
 38 GTGCTGGGACACGCACAGAAGTCCCAGGCAAACGCTCTGTCCACAGGAACTACTCCAGGCTGATTT  
 39 GCGAGATCAAATTCGCAAGAAGCCTGGGATTTTATCTGATTGAGATCTATATCCCTGCAAGCCTGATT  
 40 GTGGTGATCTCCTGGGTGAGCTTCTGGCTGCATAGGAATGCCACACCTGCTAGAGTGAGTCTGGGA  
 41 GTGACTACAGTGCTGACTATGACAACCTCTGATGAGCAGTACTAACGCACAGCTGCCTAAAATTCCTA  
 42 TATTAAGAGCATCGATGTGTTTCTGGGAACTTGCTTTGTGATGGTGTTTCGCATCCCTGCTGGAGTACG  
 43 TACTGTGGGATATCTGGGAAAAAGGATCGCCATGAGAAAATCCAGGTTTGAACAGATGAATAAGA  
 44 TGCATGAGGATCAGAAGAAAAGGCTGGCATCCCTGCCATCTCATCAACAGCAATTCTACTAGCGG  
 45 ACATCTGACAATCAGCGATAGGGGAGGGGGAGGATCTGGAGGAGCAACAGGAAACGCAGGAGTG  
 46 GGATGCCTGTCCAATAACCAGGTGGCACTGCAAAGCGGACAGCAGCAGTCCCAGATGCAGCAGCAG  
 47 CAGAGCAGTCAGGGAGGGGGAGGACTGTCCAGCACTGGAGGAACTGGAGGATGCGGAGGGGGAG  
 48 GACAGGGAGGACAGATGTCCAGCCTGAACCCTCTGAACGTGGTGACCCAGTGCAGGTGACAAGTT  
 49 GCGATCTGATCCACGGAGAGGGAGGACACTCCACCTGGTGCCTCCATCTTCCATAGCCACCATCCT  
 50 AACCAGCCTCAGAGCCAGCCACAGTCCCAGAGTCAGCCTCCATCCTCTCAGGATATTCCACCTCCAAT  
 51 TCCACCAGGACCTATTGGAATCATCAATCCATCCCTGTGCCAGCTGCTATGAACGCTAGAAACCCAA  
 52 GACAGATTATCTATAAGCATTCCACCTGTACCATCCAGGAAGCGGAGGAACTCTGCATAGAAGTGG  
 53 ACATTACGATAGAAGCTATACATGCAGCTCTCCACCTACAACTCACAGAAGCACATGTACTCTGAGG

1  
2  
3 ACTTGCAACACAGCACATATGATTTGCAATCATCCAGATTCCATTGGAAGCAGCGGAGTGCATTACCC  
4 AAGCGAAGTGAGATATAAACTGAGTGAGATGAAGACTGGAAGCAGAGGAGCAAGCTGCATCACTA  
5 CAAGCACTGGAGAACCTATTTGCTCCGGAAATCCCAGGGAGGGGAACTGGAGGATCTGGAGGAT  
6 GTGGAGCCACATCCACAACCTCCACTGATCAGCAGAAGGTCTATGGAGCAGAGCGAACCACCTCCAAC  
7 ACCTATTACAAAACACAGCACAGGAAAGTGCAAAAATCCAAATAAACTGCTGGGAGTGAGCCCATCC  
8 GATATTGATAAATACTCCAGAGTGATTTTCCCAGTGTGTTTTATTTGCTTTAATCTGATGTATTGGATT  
9 ATCTACCTGCATATCTCCAATGAACCAAACCCAGATCTGATTCAGCTGGGAAGTTGAAAGCTTACCAG  
10 CCTCAAGAACACCCGAATGGAGTCTCTAAGCTACATAATACCAACTTACACTTTACAAAATGTTGTCC  
11 CCCAAAATGTAGCCATTTCGTATCTGCTCCTAATAAAAAGAAAGTTTCTTCACATTCTAAAAAAAAAAAA  
12 AAAAAAAAAAACCCTGAGGCGCGCTCGAGGCTAGCTTGAGTATTCTATAGTGTACCT  
13 AAATAGCT  
14  
15  
16  
17

18 Color legend:

19 T7 promotor

20 Xenopus 5'UTR

21 GCCACC: KOZAK sequence

22 CDS

23 TuGluCl3 I321T: site-directed mutagenesis ATC ->ACC

24 Xenopus 3'UTR

25 SP6  
26  
27  
28  
29  
30  
31  
32  
33  
34  
35  
36  
37  
38  
39  
40  
41  
42  
43  
44  
45  
46  
47  
48  
49  
50  
51  
52  
53  
54  
55  
56  
57  
58  
59  
60

1  
2  
3 **Untangling a Gordian knot: the role of a GluCl3 I321T mutation in**  
4 **abamectin resistance in *Tetranychus urticae***  
5  
6  
7

8  
9 Wenxin Xue, Catherine Mermans, Kyriaki-Maria Papapostolou, Mantha Lamprousi,  
10 Iason-Konstantinos Christou, Emre Inak, Vassilis Douris, John Vontas, Wannes  
11 Dermauw, Thomas Van Leeuwen  
12  
13  
14  
15  
16  
17  
18  
19  
20  
21  
22  
23  
24  
25  
26  
27  
28  
29  
30  
31  
32  
33  
34  
35  
36  
37  
38  
39  
40  
41  
42  
43  
44  
45  
46  
47  
48  
49  
50  
51  
52  
53  
54  
55  
56  
57  
58  
59  
60

Supplementary Figures

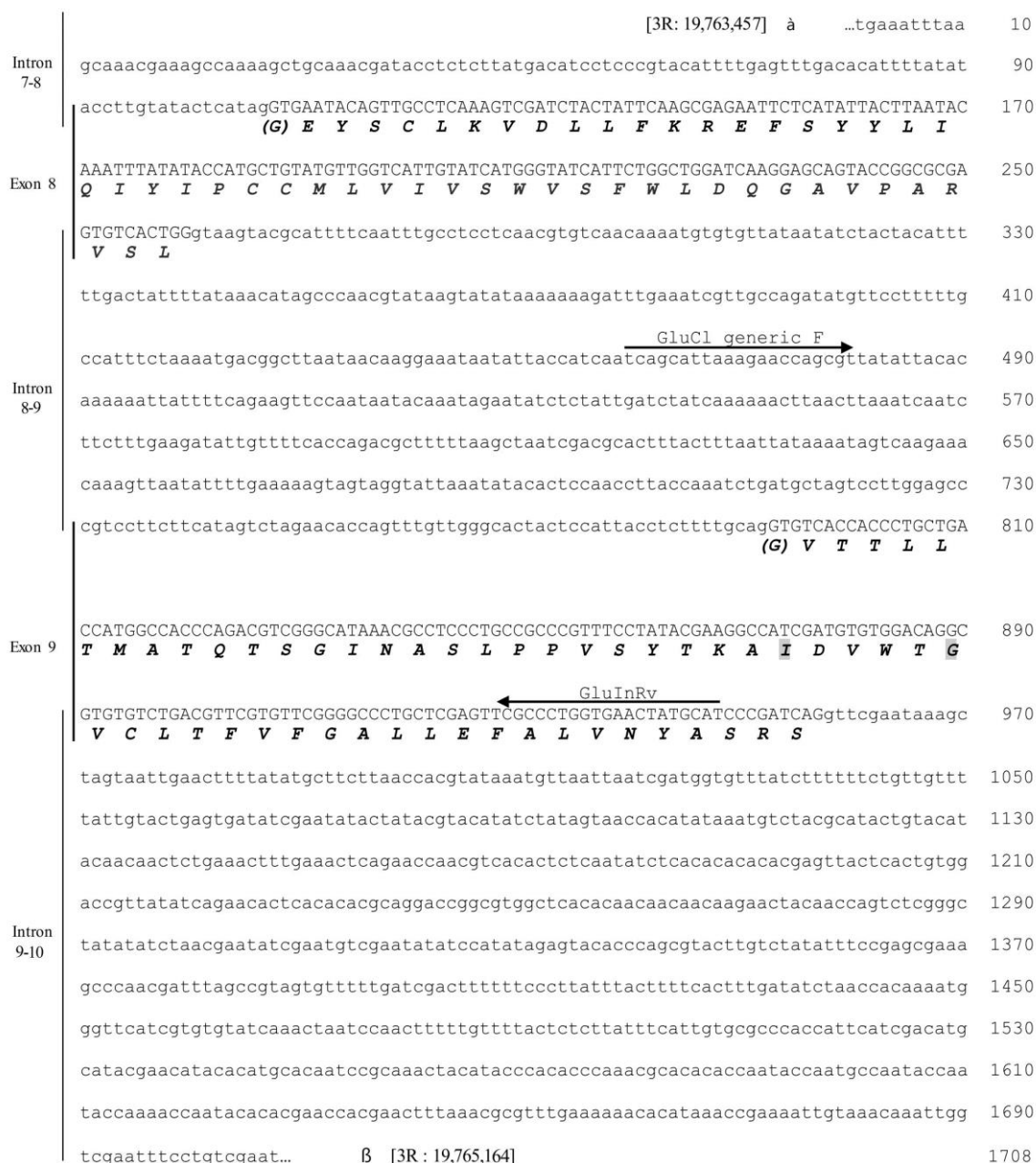


**Figure S1. *Drosophila* GluCl target region.** Nucleotide and deduced amino acid sequence of a 1708 bp fragment (region 3R: 19,763,457-19,765,164 of the BDGP6.22 genome assembly) of the *D. melanogaster* GluCl used for homology-directed repair, encompassing exon 9 that contains the target amino acid positions I307 (equivalent to I321 in Tu\_GluCl3) and G312 (equivalent to either G314 or G326 in Tu\_GluCl1 and Tu\_GluCl3 respectively), shown in light gray shading. Intron sequences are shown in lowercase letters. Horizontal arrows indicate the positions of primers GluCl\_generic\_F / GluInRV (Table S3) used for amplification and sequencing of the genome modified alleles.

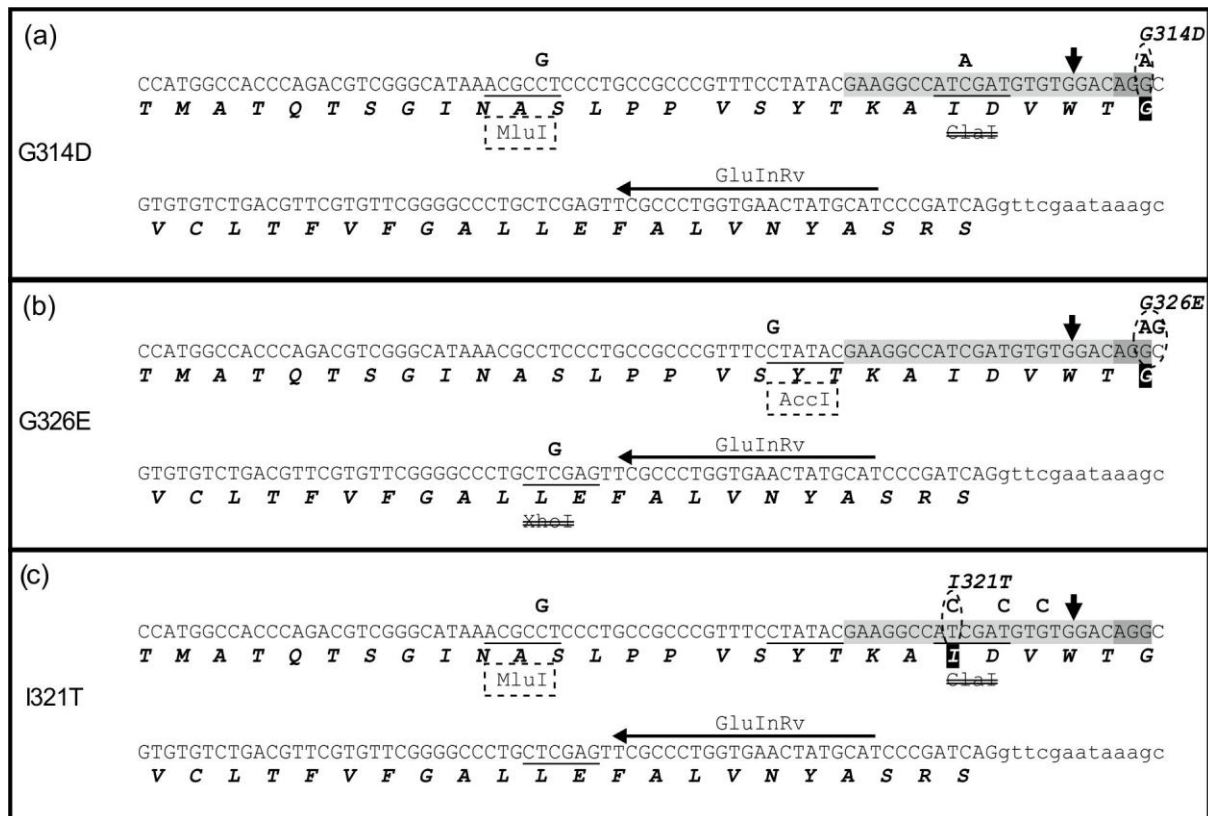


**Figure S2. CRISPR/Cas9 strategy for generation of genome modified flies.** (a): strategy for G314D mutation, (b): strategy for G326E mutation, (c): strategy for I321T mutation. All panels represent the nucleotide and deduced amino acid sequence of a 160 bp fragment of the *D. melanogaster GluCl* containing part of exon 9 (uppercase) that bears the target positions, and adjacent intron (lowercase). Light gray area indicates the CRISPR/Cas9 target selected (sgRNA), while the dark gray area indicates the corresponding PAM (-NGG) triplet. The vertical arrow denotes the break point for CRISPR/Cas9-induced double stranded break. The ovals mark the non-synonymous differences between target (wild-type) and donor (genome modified) sequences used to generate each mutation. Synonymous mutations incorporated for diagnostic purposes, as well as to avoid cleavage of the donor plasmid by the CRISPR/Cas9 machinery, are shown above the nucleotide sequence. Restriction sites abolished because of the genome modification are shown with strikethrough letters and the corresponding sequence is underlined. Restriction sites introduced because of the genome modification are shown with a dashed box and the corresponding sequence is also underlined. The horizontal arrow indicates the position of primer GluInRV (Table S3) used for sequencing of the genome modified alleles.

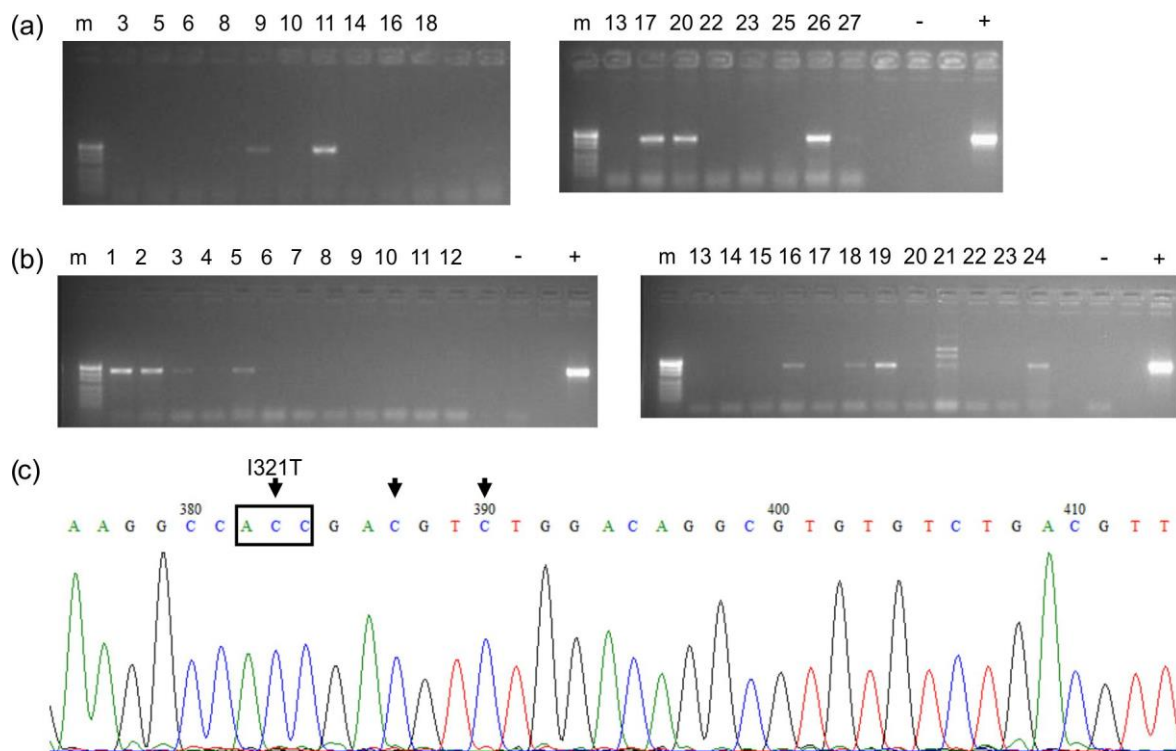


**Figure S3. Screening for genome-modified I321T flies.** (a): PCR screening following digestion with *Clal* of template DNA from pools of  $G_1$  flies derived from different  $G_0$  (injected) individuals using a specific primer combination (*GluCl\_generic\_F* / *GluCl\_specific\_R*, Table S3) that provides a diagnostic 429 bp band for the I321T mutation. (b): Screening of individual balanced  $G_2$  flies for I321T alleles using the specific primer combination (*GluCl\_generic\_F* / *GluCl\_specific\_R*, Table S3); several positive crosses are visible. m: MW marker -: nos.Cas9 DNA (negative control), +: donor plasmid template (positive control). (c): Sequencing of the relevant *GluCl* region in homozygous genome modified flies. Vertical arrows indicate modified nucleotides. The boxed ACC triplet encodes I321T.

1  
2  
3  
4  
5  
6  
7  
8  
9  
10  
11  
12  
13  
14  
15  
16  
17  
18  
19  
20  
21  
22  
23  
24  
25  
26  
27  
28  
29  
30  
31  
32  
33  
34  
35  
36  
37  
38  
39  
40  
41  
42  
43  
44  
45  
46  
47  
48  
49  
50  
51  
52  
53  
54  
55  
56  
57  
58  
59  
60

```

GluCl3_ES1  957AAAGCCACTGATGTTTGGACCGGAGCTGCCTTTTCTTTGTTTTGGTGCCCTCCTAGAGTTTGCCCTTGAAACTATGCGTCAAGA1041
GluCl3_IT1  957AAAGCCACTGATGTTTGGACCGGAGCTGCCTTTTCTTTGTTTTGGTGCCCTCCTAGAGTTTGCCCTTGAAACTATGCGTCAAGA1041
GluCl3_IT5  957AAAGCCACTGATGTTTGGACCGGAGCTGCCTTTTCTTTGTTTTGGTGCCCTCCTAGAGTTTGCCCTTGAAACTATGCGTCAAGA1041
GluCl3_IT6  957AAAGCCACTGATGTTTGGACCGGAGCTGCCTTTTCTTTGTTTTGGTGCCCTCCTAGAGTTTGCCCTTGAAACTATGCGTCAAGA1041
GluCl3_MR-VL 957AAAGCCACTGATGTTTGGACCGGAGCTGCCTTTTCTTTGTTTTGGTGCCCTCCTAGAGTTTGCCCTTGAAACTATGCGTCAAGA1041
GluCl3_TR2  957AAAGCCACTGATGTTTGGACCGGAGCTGCCTTTTCTTTGTTTTGGTGCCCTCCTAGAGTTTGCCCTTGAAACTATGCGTCAAGA1041
GluCl3_SR6  957AAAGCCACTGATGTTTGGACCGGAGCTGCCTTTTCTTTGTTTTGGTGCCCTCCTAGAGTTTGCCCTTGAAACTATGCGTCAAGA1041
GluCl3_London 957AAAGCCACTGATGTTTGGACCGGAGCTGCCTTTTCTTTGTTTTGGTGCCCTCCTAGAGTTTGCCCTTGAAACTATGCGTCAAGA1041

```

**Figure S4. Nucleotide alignment of the TM3 region of *GluCl3* of red morph *T. urticae* strains investigated in this study and a green morph *T. urticae* strain (London).** The mutation I321T (ATT-> ACT) characterized in this study in six *T. urticae* strains (IT1, IT5 IT6, ES1, MR-VL and TR2) is indicated with a red arrow and a red font. The V327G (GTC-> GCC) and L329F (CTT-> TTT) mutation found in ES1 in our previous study is indicated with a blue arrow and blue font.<sup>36</sup> The London (green font) abamectin susceptible strain originated from a wild-collected *T. urticae* population from the Vineland region (Ontario, Canada) and its TM3 *GluCl3* sequence was downloaded from the ORCAE website (<http://bioinformatics.psb.ugent.be/webtools/bogas/overview/Tetur>) with accession number *tetur10g03090*).<sup>14,73</sup> An 90% threshold was used for identity (black background) and similarity shading (grey background).



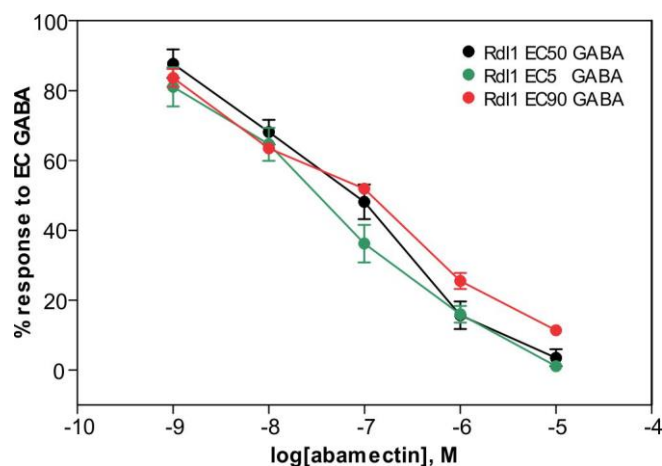
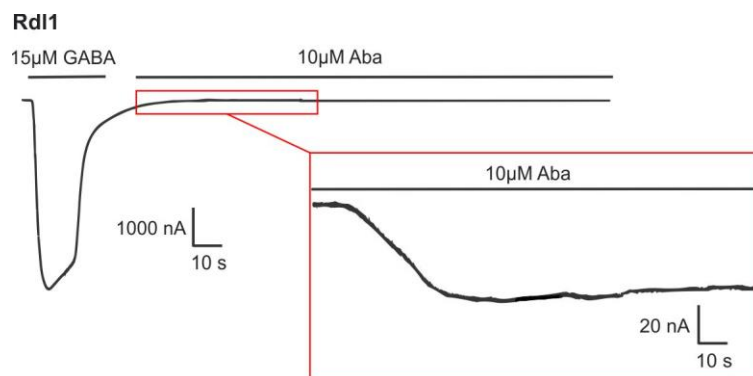


**Figure S5. Dose-response regression curve measured for abamectin obtained from oocytes expressing Rdl1 and tested with the EC<sub>5</sub>, EC<sub>50</sub> or EC<sub>90</sub> of GABA. Error bars indicate SEM (n=8).**



15  
16  
17  
18  
19  
20  
21  
22  
23  
24  
25  
26  
27  
28  
29  
30  
31  
32  
33  
34  
35  
36  
37  
38  
39  
40  
41  
42  
43  
44  
45  
46  
47  
48  
49  
50  
51  
52  
53  
54  
55  
56  
57  
58  
59  
60

**Figure S6. Detail of a current trace when abamectin was administered to Rdl1 expressing oocytes.**

For Peer Review

1  
2  
3 **Untangling a Gordian knot: the role of a GluCl3 I321T mutation in**  
4 **abamectin resistance in *Tetranychus urticae***  
5  
6  
7

8  
9 Wenxin Xue, Catherine Mermans, Kyriaki-Maria Papapostolou, Mantha Lamprousi,  
10 Iason-Konstantinos Christou, Emre Inak, Vassilis Douris, John Vontas, Wannes  
11 Dermauw, Thomas Van Leeuwen  
12  
13  
14  
15  
16  
17  
18  
19  
20  
21  
22  
23  
24  
25  
26  
27  
28  
29  
30  
31  
32  
33  
34  
35  
36  
37  
38  
39  
40  
41  
42  
43  
44  
45  
46  
47  
48  
49  
50  
51  
52  
53  
54  
55  
56  
57  
58  
59  
60

Supplementary Tables

**Table S1. *T. urticae* populations used in this study**

Strain	DOC <sup>a</sup>	Origin	Host plant	Reference
IT1	06/2017	Granieri, Italy	Carnation	Xue et al. 2020
IT5	05/2018	Granieri, Italy	Carnation	
IT6	05/2018	Vittoria, Italy	Gerbera	
ES1	05/2017	Sevilla, Spain	Strawberry	
MR-VL	2005	Gent, Belgium	poplar cuttings, beans or ornamentals	Van Leeuwen et al., 2005 (fenbutatin oxide selection line)
TR2	11/2017	Mersin, Turkey	Zucchini	İnak et al., 2019
SR6	2017	Italy	Tomato	This Study

<sup>a</sup>Date of collection

**Table S2. *GluCl1/2/3/4/5* TM3 and *Rdl1/2/3* TM2/TM3 region genotypes and abamectin resistance in the surveyed *T. urticae* populations**

Strain	GluCIs	RdIs	Abamectin		
			Slope(±SE)	LC50s (95% CI)/ mg L <sup>-1</sup>	RRs <sup>a,b</sup> (95%CI)
IT1	I321T in <i>GluCl3</i>	-	3.31 (±0.32)	14.64 (12.08-17.12)	61.00 (50.33-71.33)*
IT5	I321T in <i>GluCl3</i>	-	4.28 (±0.13)	14.26 (12.45-16.15)	59.42 (51.88-67.29)*
IT6	I321T in <i>GluCl3</i>	-	3.33 (±0.22)	24.96 (22.76-27.20)	104.0 (94.8-113.3)*
ES1	I321T/V327G/L329F in <i>GluCl3</i>	-	2.53 (±0.18)	78.59 (67.63-90.84)	327.5 (281.8-378.5)*
MR-VL	I321T in <i>GluCl3</i>	-	3.78 (±0.28)	1.79 (1.66-2.12)	7.46 (6.92-8.83)*
TR2	I321T in <i>GluCl3</i>	-	2.52 (±0.25)	11.19 (8.57-14.50)	46.63 (35.71-55.77)*
SR6	-	-	3.31 (±0.25)	0.24 (0.21-0.26)	1.00

<sup>a</sup>Resistance Ratios compared to the susceptible strain SR6

<sup>b</sup>An asterisk (\*) indicates the RR was considered significantly different from 1 based on non-overlap of 95% CI (PoloPlus LeOra Software).<sup>50</sup>

**Table S3. Primers used in this study**

Primer Name	Sequence (5' - 3')	Use
Tu_GluCl1_dia_F	TTGGATTGACCCTAACTCAGCA	
Tu_GluCl1_dia_R	TTGCACCAACAATTCCTTGA	
Tu_GluCl2_dia_F	TCATCGTCTCTTGGGTCTCC	
Tu_GluCl2_dia_R	CCCATCGTCGTTGATACCTT	
Tu_GluCl3_dia_F	CCGGGTCAGTCTTGGTGTTA	survey of TM3 region of GluCl3 (Dermauw et al. 2012)
Tu_GluCl3_dia_R	CACCACCAAGAACCTGTTGA	
Tu_GluCl4_dia_F	TATTCCAGCCCGAGTTTCAC	
Tu_GluCl4_dia_R	AATCGGAGGTTGACTTGGTG	
Tu_GluCl5_dia_F	ATGTTGGTCATCGTTTCGTG	
Tu_GluCl5_dia_R	AATCGGGATTGAATTTGCTG	
Tu_Rdl1_TM3F	TGCGAAATTCAGTTGACTCG	
Tu_Rdl1_TM3R	CCAATTGTTGGAAGCGATTT	
Tu_Rdl2_TM3F	CCTGCAAGCCTTATAGTGGTG	survey of TM2/TM3 region of Rdl3
Tu_Rdl2_TM3R	CACTTTGTTCCGGCTACAGCA	
Tu_Rdl3_TM3F	TCCCTGCCAGCCTTATAGTG	
Tu_Rdl3_TM3R	ATGGCAATCCGTTTACCAAG	
sgRNA sense	CTTCGAAGGCCATCGATGTGTGGAC	sgRNA
sgRNA antisense	AAACGTCCACACATCGATGGCCTTC	
GluExFw	TGGATGGCATTCTCTGTACCT	Genomic region amplification / sequencing
GluExRv	GCAAGGAACCGAACAATCGT	
GluInFw	ACCTAACCCTTTTGCAGGT	Genomic region sequencing
GluInRv	ATGCATAGTTCACCAGGGCG	
GluCl_generic_F	TCAGCATTAAAGAACCAGCGT	Sequencing, allele screening
GluCl_specific_R	CACGCCTGTCCAGACGTCGG	